Anfossi, D. et al. (2003) *Plume Rise*. Chapter 6 of *AIR QUALITY MODELING - Theories, Methodologies, Computational Techniques, and Available Databases and Software. Vol. I - Fundamentals* (P. Zannetti, Editor). Published by The EnviroComp Institute (http://www.envirocomp.org/) and the Air & Waste Management Association (http://www.awma.org/).

Chapter 6

Plume Rise

Domenico Anfossi [(1)], Elisa Canepa [(2)] and Han van Dop [(3)]

[(1)] *CNR Istituto di Scienze dell'Atmosfera e del Clima, Corso Fiume 4, I-10133 Torino, Italy*
anfossi@to.infn.it
[(2)] *INFM (National Institute for the Physics of Matter), Department of Physics - University of Genova, Via Dodecaneso 33, I-16146 Genova, Italy*
canepae@fisica.unige.it
[(3)] *Institute for Marine and Atmospheric Research Utrecht, P.O. box 80.005, 3508 TA Utrecht, The Netherlands*
dop@phys.uu.nl

Abstract: Plume rise determination is one of the main processes encountered in air pollution modeling. Therefore, the most commonly used methods for introducing plume rise in dispersion models are presented. They encompass simple but robust and documented semi empirical formulations, easy to be implemented in operative models, and advanced plume rise models. Then, the problem of how to account for plume rise in Lagrangian dispersion particle models is addressed. Finally, special situations of plume rise, like the occurrence of an elevated inversion, or the presence of building and/or stacks features interacting with the plume, are investigated.

Key Words: buoyant plumes, jet plumes, ambient turbulence, self-induced turbulence, dispersion modeling, effective plume heights, stability conditions.

List of Symbols

A	dimensional constant in Equation (57) [$L^{3/4}\ M^{-1/4}\ T^{-1/4}$]
A_i	drift coefficient for velocity in Equations (97) [$L\ T^{-2}$]
A_p	dimensionless constant in Equation (87)
A_s	stack outlet area [L^2]
A_1	dimensional constant in Equation (36) [$T^{6/5}\ L^{-6/5}$]
A_2	dimensional constant in Equation (36) [$T^{6/5}\ L^{-3/5}$]
A_3	dimensional constant in Equation (37) [$T^{15/8}\ L^{-3/2}$]
A_4	dimensional constant in Equation (37) [$T^{6/5}\ L^{-3/5}$]
A^{ϑ}	drift coefficient for potential temperature in Equations (97) [$K\ T^{-1}$]
a	drift coefficient in Equation (77) [$L\ T^{-2}$]
B	plume particle buoyancy [$L\ T^{-2}$]
B_0	initial plume buoyancy [$L\ T^{-2}$]
b_i	acceleration of air displaced through an inversion [$L\ T^2$]
b_{ij}	diffusion coefficient for velocity in Equations (97) [$L\ T^{-3/2}$]
b_p	lower edge of the plume [L]
b^{ϑ}	diffusion coefficient for potential temperature in Equations (97) [$K\ T^{-1/2}$]
C	parameter in Equation (138) [$L^{-1/3}\ T$]
C_0	dimensionless constant in Equation (77)
c_B	dimensional constant in Equations (92) [$L^2\ T^{-5}$]
c_p	specific heat at constant pressure [$L^2\ T^{-2}\ K^{-1}$]
c_w	dimensional constant in Equations (92) [$L^2\ T^{-3}$]
c_1	dimensionless constant in Equations (91)
c_2	dimensionless constant in Equations (91)
D	dimensionless parameter in Equation (139)
D_0	dimensional constant in Equation (57) [L]
D_1	dimensionless constant in Equation (57)
D_2	dimensional constant in Equation (57) [T K]
d	spacing between adjacent stacks [L]
d_s	internal diameter of the stack outlet [L]
d_1	dimensionless constant in Equation (70)
d_2	dimensionless constant in Equation (70)
d_3	dimensionless constant in Equation (71)
d_4	dimensionless constant in Equation (72)
dW	random increment in Equation (77)
$d\omega_B$	random increments for buoyancy in Equations (84) [$T^{1/2}$]
$d\omega_j$	random increments for velocity in Equations (97) [$T^{1/2}$]
$d\omega_w$	random increments for velocity in Equations (84) [$T^{1/2}$]
$d\omega^{\vartheta}$	random increments for potential temperature in Equations (84) [$T^{1/2}$]

E	turbulent kinetic energy [$L^2\ T^{-2}$]
E_n	dimensionless enhancement factor
f	dimensionless stack tip downwash correction factor
f'	dimensionless fraction of the plume trapped below inversion
f_b	atmospheric turbulence buffet frequency [T^{-1}]
F_b	buoyancy flux parameter [$L^4\ T^{-3}$]
F_b^i	buoyancy flux of i-th particle [$L^4\ T^{-3}$]
F_e	plume buoyancy flux at the end of bending-over phase [$L^4\ T^{-3}$]
F_j	buoyancy of the j-th stack [$L^4\ T^{-3}$]
F_m	momentum flux parameter [$L^4\ T^{-2}$]
F_{m*}	dimensionless momentum flux
F_m^i	momentum flux of i-th particle [$L^4\ T^{-3}$]
F_r	dimensionless Froude number
F_*	dimensionless buoyancy flux
G	plume volume in Equations (79) [$L^3\ T^{-1}$]
G_s	G value at stack outlet [$L^3\ T^{-1}$]
g	acceleration due to gravity [$L\ T^{-2}$]
k_v	dimensionless added mass
H	upward surface sensible heat flux times $g/(c_p \rho_a \vartheta)$ [$L^2\ T^{-3}$]
H^*	dimensional parameter in Equation (57) [L]
H_b	building height [L]
H_i	merging point height in Equation (138) [L]
H_j	height of the j-th stack in Equation (138) [L]
$H_{\max}$	highest stack in Equation (139) [L]
$H_{\min}$	lowest stack in Equation (139) [L]
h	mixing height [L]
h'	inversion height with respect to stack top [L]
h_e	effective stack height [L]
h_t	height of the base of atmospheric thermal discontinuity [L]
L_b	buoyancy length scale [L]
L_e	effective length [L]
L_m	momentum length scale [L]
M_e	plume momentum flux at the end of bending-over phase [$L^4\ T^{-2}$]
N	Brunt-Väisälä frequency [T^{-1}]
N'	modified Brunt-Väisälä frequency [T^{-1}]
n	dimensionless number of stacks
P_b	dimensionless buoyancy flux in Equation (127)
P_s	dimensionless buoyancy flux in Equation (136)
Q_f	total heat release rate of a flare [$M\ L^2\ T^{-3}$]
Q_h	stack effluent heat emission rate [$M\ L^2\ T^{-3}$]
Q_m	stack effluent mass emission rate [$M\ T^{-1}$]
R	plume radius [L]

R_e	plume radius at end of bending-over phase [L]
R_s	dimensionless initial plume radius
R_0	dilution radius [L]
r_a	radius of air eddies [L]
r_s	internal radius (or equivalent radius) of the stack outlet [L]
S_{wa}^3	third moment of ambient Eulerian PDF [L^3 T^{-3}]
S	dimensionless parameter in Equation (137)
s	stability parameter [T^{-2}]
s_c	distance along the centerline [L]
T_a	ambient temperature [K]
T_{a0}	ambient temperature at stack outlet height [K]
T_e	Eulerian time scale [T]
T_m	Lagrangian time scale in Equation (90) [T]
T_{s0}	temperature of stack effluent at stack outlet [K]
T_p	Lagrangian time scale of the plume [T]
t	travel time [T]
t_p	upper edge of the plume [L]
t_0	initial turbulent timescale of the plume particle [T]
U_a	wind speed that can vary with height [L T^{-1}]
U_i	particle velocity component (i = 1, 2, 3) [L T^{-1}]
U_{sc}	velocity along the centerline [L T^{-1}]
$U_z(t)$	mean vertical wind component [L T^{-1}]
u	mean uniform horizontal wind speed in Equation (59) [L T^{-1}]
u_p	horizontal particle velocity [L T^{-1}]
$u'(t)$	turbulent velocity fluctuation in Equation (77) [L T^{-1}]
u_*	friction velocity [L T^{-1}]
u_0	mean wind speed at the stack outlet height [L T^{-1}]
u_5	wind speed at the 1.5 z_s [L T^{-1}]
v_a'	r.m.s. velocity of an air eddy with respect to the plume [L T^{-1}]
v_{s0}	effluent emission speed at stack outlet [L T^{-1}]
v_a	relative velocity of two particles [L T^{-1}]
v_e	entrainment velocity [L T^{-1}]
W	vertical velocity of the plume [L T^{-1}]
w_b	buoyancy contribution to the vertical velocity [L T^{-1}]
w_m	momentum contribution to the vertical velocity [L T^{-1}]
w_p	vertical velocity of the particle [L T^{-1}]
$w'(t)$	turbulent velocity fluctuation in Equation (66) [L T^{-1}]
w_*	convective velocity scale [L T^{-1}]
X_i	particle position component (i = 1, 2, 3) [L]
X_*	dimensionless downwind distance
X_z	plume particle's vertical position [L]
x	downwind distance from stack [L]
x_*	function of downwind distance from Equation (56) [L]

x_c^*	critical distance defined by Equation (36) [L]
x_f	downwind distance of maximum plume rise [L]
x_T	length defined by Equation (56) [L]
y	lateral space coordinate or radial distance from axis [L]
z	elevation a.g.l. [L]
z'_{eq}	equilibrium height with respect to the stack top [L]
z_s	stack height [L]
α	dimensionless constant in Equations (79)
α_B	dimensionless constant in Equations (92)
α_v	dimensionless constant in Section (4.3.3)
α_w	dimensionless constant in Equations (92)
β	dimensionless classic entrainment parameter
β_1	dimensionless neutral entrainment parameter in Equation (116)
β_2	dimensionless stable entrainment parameter in Equation (117)
β_j	dimensionless jet entrainment parameter in Equation (116)
γ	dimensionless constant in Equations (79)
γ_1	dimensionless constant in Equation (80)
γ_2	dimensionless constant in Equation (82)
$\Delta H_{\min}$	maximum single plume rise from lowest stack in Equation (139) [L]
ΔH^N	final rise for merged plumes [L]
Δh	final plume rise [L]
$\Delta h(t)$	plume rise as a function of travel time [L]
$\Delta h(x)$	plume rise as a function of distance downwind of stack [L]
$\Delta h'$	final plume rise corrected for the stack tip downwash [L]
$\Delta h''$	actual plume rise in Equation (123) [L]
Δh_d	plume rise of a building downwashed plume [L]
Δh_i	thickness of the inversion layer [L]
Δh_1	plume rise from a single stack in multiple sources [L]
Δh_{max}	maximum plume rise [L]
ΔT_c	critical temperature difference [K]
ΔT_0	temperature difference between air and plume at the stack outlet [K]
Δt	time step [T]
Δu	difference in the horizontal velocity between the plume and the ambient environment [L T^{-1}]
Δz	vertical increment [L]
$\Delta \vartheta^*$	dimensional parameter in Equation (57) [K]
$\Delta \vartheta_i$	potential temperature jump of the inversion [K]
$\Delta \vartheta_m$	maximum excess temperature [K]
$\Delta \vartheta_{100}$	potential temperature variation over 100 m in Section 2.7.1 [K]
δ	dimensionless parameter in Equation (133)

$\partial\vartheta/\partial z$	vertical gradient of absolute potential temperature [K L^{-1}]
ε_a	ambient rate of dissipation of turbulent kinetic energy [L^2 T^{-3}]
ε_B	dissipation rate of buoyancy of the plume particle [L^2 T^{-5}]
ε_m	dissipation rate in Equation (96) [L^2 T^{-3}]
ε_p	rate of dissipation of turbulent kinetic energy in the plume [L^2 T^{-3}]
ε_w	dissipation rate of velocity of the plume particle [L^2 T^{-3}]
λ	dimensionless parameter in Equation (132)
η_{eq}	dimensionless parameter in Equation (133)
ϕ	angle between the horizontal and the centerline [deg]
μ_a	air molecular weight [M mol^{-1}]
μ_s	emission molecular weight [M mol^{-1}]
ρ_a	density of ambient atmosphere [M L^{-3}]
ρ_{a0}	ambient density at stack outlet height [M L^{-3}]
ρ_s	density of effluent [M L^{-3}]
ρ_{s0}	density of effluent at stack outlet [M L^{-3}]
σ_{y0}	enhanced horizontal dispersion coefficient [L]
σ_z	plume width [L]
σ_{z0}	enhanced vertical dispersion coefficient [L]
σ_{up}^2	longitudinal velocity variance due to the plume rise [L^2 T^{-2}]
σ_{vp}^2	crosswind velocity variance due to the plume rise [L^2 T^{-2}]
σ_{wa}^2	second moment of ambient Eulerian PDF [L^2 T^{-2}]
σ_w^2	vertical wind velocity variance [L^2 T^{-2}]
σ_{wp}^2	vertical velocity variance due to the plume rise [L^2 T^{-2}]
ϑ_a	ambient potential temperature [K]
ϑ_p	potential temperature of the plume particle [K]
τ	dimensionless travel time

1 Introduction

The behavior of a chimney plume in the atmosphere is a rather complex process, which is influenced by the emission characteristics, the nearby terrain features, the actual wind profiles, stratification (vertical gradient of potential temperature) and turbulence. Basically, plumes emitted into the atmosphere rise under the action of their initial momentum and buoyancy (if they possess a temperature which is greater than the ambient temperature). For power plants and other moderate-to-large industrial sources, the major contribution to the rise is from the heat flux. For example, a modern power plant typically discharges ≈ 100 MW of heat from its stack. These are called buoyant plumes. In such conditions plumes can rise for hundreds of meters. Initial momentum can be important for smaller

sources, with little or no buoyancy, such as those typically found in light manufacturing. Plumes from these sources are referred to as jet plumes.

A jet plume, moving through the ambient atmosphere, experiences a shear force at its perimeter, where momentum is transferred from the jet to the surrounding air. This causes an increase of the plume diameter and a decrease of its velocity. This phenomenon is known as entrainment. In a buoyant plume, air is entrained in the same way as in a jet and the buoyancy forces help maintain the motion of the plume as it transfers momentum to the surrounding air. For this reason, buoyant plumes generally rise higher than jet plumes. The entrained ambient air mixes with the plume air, thus diluting the plume components before they reach ground level and, in the case of buoyant plumes, decreasing the average temperature difference between air and plume. In a calm atmosphere, plumes rise almost vertically, whereas in windy situations they bend over. In this case, the velocity of any plume parcel is the vector composition of horizontal wind velocity and vertical plume velocity in the first stage and then approaches the horizontal wind velocity.

The motion of bent over plumes can be schematically divided into three phases (Slawson and Csanady, 1967; 1971): an initial phase, in which the self-generated turbulence, due to the action of their mechanical and thermal energy, prevails; an intermediate phase, where the ambient turbulence in the inertial sub-range is important; a final phase, in which the main mechanism is the mixing due to the large atmospheric energy containing eddies (see Figure 1).

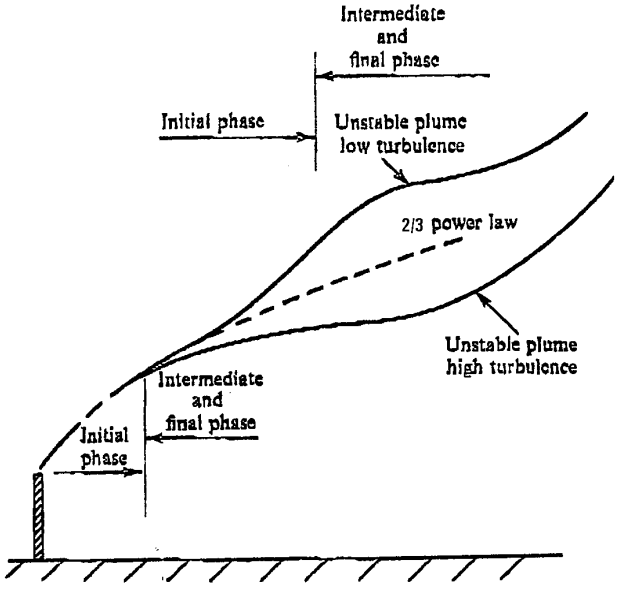

Figure 1. Two possibilities of unstable plume behavior (adapted from Slawson and Csanady, 1971). [Reprinted with permission from Cambridge University Press]

Effective plume height h_e (elevation of plume centerline relative to ground level) results from the sum of stack height z_s and plume rise Δh (Figure 2)

$$h_e = z_s + \Delta h \tag{1}$$

Thus, a correct estimation of buoyant plume rise is one of the basic requirements for the determination of ground level concentrations of airborne pollutant emitted by industrial stacks. In fact maximum ground level concentration is roughly inversely proportional to the square of the final height h_e. For this reason, in many

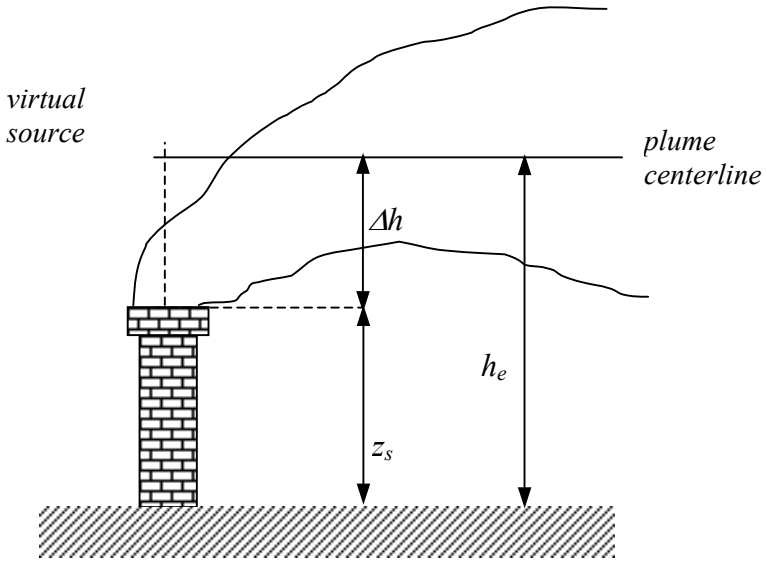

Figure 2. The plume rise: schematic representation.

simple dispersion models, stack gases are assumed to be emitted from a virtual source located at a height h_e (see Figure 2) along the vertical above the stack.

The description of plume rise is based on the fluid dynamic equations, namely on the mass, momentum and energy conservation equations. A complete, exhaustive theory is not yet available. Therefore some simplifying assumptions need to be made. These will give rise to simplified models that can just take into account the main variables of the examined case.

Plume rise formulae can be ranked either empirical or theoretical, but the distinction is not so clear:

- the empirical formulae are based almost exclusively on experimental data both for their numerical parameters and for their functional form
- the theoretical formulae, in spite of including some parameters with an experimental origin, have a functional form based on the solution of equations expressing laws of mass, momentum and energy conservation

Some formulae provide the plume rise as a function of the distance, but most of them provide a constant value (final plume rise) that the plume reaches at a large downwind distance. These formulae contain height depending atmospheric variables normally specified at the stack outlet height.

Several studies and review works have provided semi-empirical formulae for evaluating Δh (e.g., Holland, 1953; Brummage, 1966; Bringfelt, 1969; Fay et al., 1970; Carpenter et al., 1971; Briggs, 1975; Strom, 1976; Hanna et al., 1982; and many others); others have provided more complex and comprehensive descriptions of several physical interactions between the plume and the ambient air (e.g., Golay, 1982; Netterville, 1990). Relevant and exhaustive review papers on the plume rise subject can be found in the literature, such as, for instance, Briggs (1975) and Weil (1988). In this chapter, we will utilize a great deal of material from these reviews.

For many specific applications, literature supplies functional forms and empirically determined parameters, but such models may provide wildly inaccurate results, if they are used beyond the context where they have been obtained. In uncertain cases, Briggs (1975) recommends to use, in the application, the formula that provides the minimum plume rise; this result is "the most conservative", since it gives rise to the maximum values of concentration expected at the ground, thus limiting the risk of a possible underestimation. It is hard to specify clearly the accuracy of plume rise formulae: some discordance up to 25% between the observed and the expected value are not unusual.

This chapter, which is concerned with plume rise from continuous releases, focuses on:

- semi-empirical formulations
- advanced plume rise models
- particle models for plume rise
- special cases (like building downwash, penetration of elevated inversion, multiple source, flare stacks, fires and so on)

The semi-empirical formulations, expressed as analytical relationships, have a functional form obtained from the solution of mass, momentum and energy conservation equations in simplified conditions (such as steady conditions, uniform wind and stability) and their numerical parameters are generally deduced from experimental data. These are the plume rise estimations mostly used in regulatory model applications.

In the advanced plume rise models the conservation equations are numerically integrated, thus giving practical solutions for varying winds and thermal structure. Due to present days computer capabilities, these models may also be used for regulatory applications. However it cannot be automatically accepted that these fully 3D models always yield results better than simpler models due to the

difficulty, in some applications to real cases, of getting the needed input data with the necessary time and space resolution.

The particle models for plume rise are relatively new methods, not yet widely used for regulatory purposes. We think that it is important to present and discuss them in some detail since the Lagrangian approach is a more natural way of describing the dispersion process (Sawford, 1985). Furthermore these are probably the methods of the future and allow a high resolution, particularly the small time behavior of plume dispersion (Nguyen et al., 1997)

The section on special cases covers many aspects of the plume rise phenomenon that are of practical importance in many applications.

Our discussion of plume rise addresses fundamental aspects and major problems, but it is not exhaustive. We intend neither to make any ranking of the models presented in the next sections, nor to recommend which model is the best for a specific application, because we want to avoid any subjective judgment which may be also influenced by the particular national regulatory laws. We wish to present a review of updated and validated existing techniques that can be used by modelers according to their specific needs. Even if no guidance is given whether a reader should use one of the models out of those suggested for a specific problem, the general rule might be to preferably use those formulas, if any, that are validated, recommended or suggested by National Environmental Protection Agencies. Being used and tested by hundreds of users, these models will, at least, guarantee that the major bugs and/or uncertainties were identified and amended and unrealistic results avoided.

2 Semi-Empirical Formulations

2.1 Governing Equations

As above anticipated, the differential equations expressing the conservation of the total fluxes of mass, momentum, and energy through a plume cross section (e.g., Morton et al., 1956; Briggs 1975; Weil, 1988) are the basis of all the analytical plume rise models. These equations are closed using the entrainment assumption (Morton et al., 1956), which prescribes that the entrainment velocity, i.e. the rate at which ambient air is entrained into the plume, is proportional to the mean local rise velocity. It may be worth mentioning that Priestley (1956) provided an alternative entrainment assumption, based on energy arguments, that gives the same basic plume rise results as Morton et al. (1956).

The following simplifications are made: the plume rises in a steady, horizontal wind of constant direction and variable with height speed $U_a(z)$; stratification, if present, is constant with the height; plume cross section is circular with radius R; plume properties (mass, velocity, temperature) have a “top hat” distribution (that

is to say in each section the cited quantities are constant inside the plume and null outside); the plume pressure is the same as in the local environment; the density differences are sufficiently small to allow making the Boussinesq approximation; since the efflux volume quickly mixes with a large volume of ambient air, the effluent has the same molecular weight and specific heat as air.

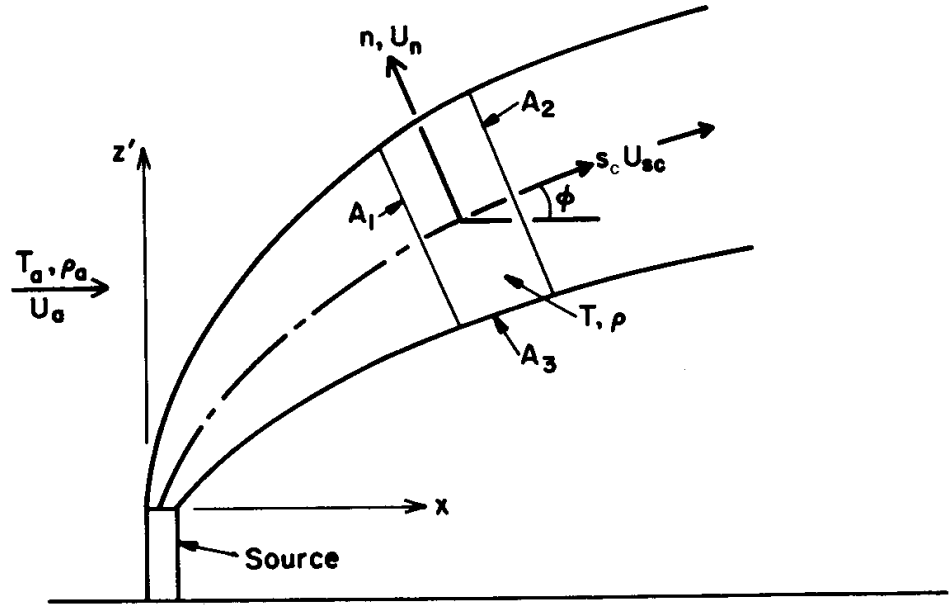

Figure 3. Schematic and nomenclature for plume in a crosswind (adapted from Weil, 1988). [Reprinted with permission from American Meteorological Society].

In the case of a crosswind, conservation of mass, horizontal momentum, vertical momentum and energy are given respectively by (Weil, 1988)

$$\frac{d}{ds_c}\left(U_{sc}R^2\right) = 2R\beta W \tag{2}$$

$$\frac{d}{ds_c}\left(U_{sc}R^2\Delta u\right) = -R^2 W\frac{dU_a}{dz} \tag{3}$$

$$\frac{d}{ds_c}\left(U_{sc}R^2 W\right) = gR^2\frac{\left(\rho_a-\rho_s\right)}{\rho_s} \tag{4}$$

$$\frac{dF_b}{ds_c} = sWR^2 \tag{5}$$

where (see also Figure 3): s_c and U_{sc} are the distance and velocity along the centerline, β is the dimensionless entrainment parameter, W is the plume vertical velocity, Δu is the difference in the horizontal velocity between the plume and the ambient environment, g is the acceleration due to gravity, ρ_a and ρ_s are the air and plume density, respectively, F_b is the buoyancy flux defined by

$$F_b = U_{sc} R^2 g \frac{(\rho_a - \rho_s)}{\rho_a} \tag{6}$$

and s is the stability parameter defined by

$$s = \frac{g}{\vartheta_a} \frac{\partial \vartheta_a}{\partial z} \tag{7}$$

ϑ_a being the potential temperature of the air and $\partial \vartheta_a / \partial z$ its vertical gradient.
The plume trajectory, $\Delta h(x)$, can be obtained from the above equations and from the following relationships (kinematic conditions)

$$\frac{d\Delta h}{ds_c} = \frac{W}{U_{sc}}, \qquad \frac{dx}{ds_c} = \frac{U_a + \Delta u}{U_{sc}} \tag{8}$$

For sake of completeness, and for reference to previous and/or related work on the plume rise, the following remarks may be important.

F_b is related to the heat emission rate Q_h by the following relationship

$$F_b = g Q_h / \pi c_p \rho_a T_a \tag{9}$$

where T_a = temperature of the air;
c_p = specific heat of air at constant pressure.

Q_h is given by the following equation

$$Q_h = Q_m c_p (T_{s0} - T_{a0}) \tag{10}$$

where Q_m = effluent mass emission rate;
T_{s0} = absolute temperature of effluent at stack outlet;
T_{a0} = absolute temperature of ambient atmosphere at stack outlet height.

Q_m may be expressed in terms of other variables as follows

$$Q_m = \rho_{s0} A_s v_{s0} \tag{11}$$

where ρ_{s0} = mass density of effluent at stack outlet;
A_s = stack outlet area;
v_{s0} = effluent emission speed at stack outlet.

Using Equation (11) and the following equality

$$\rho_{s0}(T_{s0} - T_{a0}) = T_{a0}(\rho_{a0} - \rho_{s0}) \tag{12}$$

Q_h can be expressed in terms of the mass density of ambient air at stack outlet height, ρ_{a0}, and of the pollutants, ρ_{s0}, as follows

$$Q_h = A_s v_{s0} T_{a0} c_p (\rho_{a0} - \rho_{s0}) \tag{13}$$

In the plume rise formulae for jet plumes, where the initial momentum plays the major role in the rising process, F_b is substituted by the momentum flux F_m, given by the following equation

$$F_m = v_{s0}^2 \frac{A_s \rho_{s0}}{\pi \rho_{a0}} \tag{14}$$

Notice that the buoyancy and momentum fluxes - Equations (6) and (14) - by convention are divided by π. This convention derives (Briggs, 1984) from the assumption of round top hat profile of all the plume quantities in the early plume rise studies. This assumption leads to the presence of π on both sides of the flux conservation equations.

In some plume rise formulations (e.g., Hewett et al., 1971), the buoyancy flux is defined by $F_b = U_{sc} R^2 g(\rho_a - \rho_s)/\rho_s$. According to Briggs (1972), this definition is equivalent to assuming that the buoyant force acts on a fluid of density ρ_s. However, the density of the fluid driven by the buoyant force is better approximated by ρ_a, since a turbulent plume is made up mostly of entrained fluid (Briggs, 1984).

In some formulae, the Brunt-Väisälä frequency, *N,* defined as

$$N = +\sqrt{s} \tag{15}$$

is used instead of the stability parameter *s* - see Equation (7). In stable conditions, the Brunt-Väisälä frequency is the natural frequency of oscillation of a fluid particle if perturbed from its equilibrium position; for plumes, N^{-1} is the time

scale for the depletion of the buoyancy flux and for the maximum rise in a stable environment (in the atmosphere a typical value of N^{-1} is 1 min).

The formulae that are going to be presented in the following sections are mostly, but not exclusively, derived from Briggs (1969, 1972, 1975, 1984). Briggs formulae, together with some new result recently appeared in the literature due to other authors, have been incorporated into most of the U.S. EPA models (http://www.epa.gov/scram001/t22.htm). These formulae represent a reasonable compromise between accuracy and simplicity, even though, according to many (e.g., Henderson-Sellers and Allen, 1985), they may tend to overestimate the plume rise at large downwind distances. Note that some authors (Strom, 1976; Hanna, 1994) suggest, in the absence of particular expressions derived for specific problems, using Briggs formulae.

It is worthwhile pointing out that Manins (1985) summarized evidence (from large fires, volcanic eruptions and clouds from thermonuclear explosions) showing that the vertical plume rise equation derived in the next section - Equation (45) - holds for over four orders of magnitude variation in rise height.

2.2 Plume Rise in the Transitional Phase

By solving the system of equations presented in Section 2.1, simple analytical expressions, easy to use in dispersion models, can be achieved.

2.2.1 Neutral and Unstable Case

Let us firstly consider the rise of a bent over plume in neutral conditions ($s = 0$) and uniform wind (no shear) and neglect ambient turbulence. At some distance from the source, plume can be considered as nearly horizontal and the following approximations can be made: $U_{sc} \cong U_a = const$ and $W << U_a$. From Equation (2) it follows that the plume radius grows linearly with height. In these stability conditions, Equation (5) implies that the buoyancy flux F_b is conserved. Thus, F_b is expressed by means of its value at the stack outlet, in terms of, respectively, temperatures and densities

$$F_b = g\, v_{s0}\, \frac{A_s \left(T_{s0} - T_{a0}\right)}{\pi \qquad T_{s0}} \tag{16}$$

$$F_b = g\, v_{s0}\, \frac{A_s \left(\rho_{a0} - \rho_{s0}\right)}{\pi \qquad \rho_{a0}} \tag{17}$$

Similarly, F_m is expressed by

$$F_m = v_{s0}^2 r_s^2 \frac{T_{a0}}{T_{s0}} \tag{18}$$

$$F_m = v_{s0}^2 r_s^2 \frac{\rho_{s0}}{\rho_{a0}} \tag{19}$$

where r_s is the internal radius of the stack outlet.

Note that, usually, in Equations (16) and (17), instead of A_s, we find r_s (or, for a non-circular stack having an area A_s, the equivalent radius given by $r_s = \sqrt{A_s/\pi}$). It may be worth pointing out that for the emissions whose molecular weight, μ_s, differs considerably from the air molecular weight, μ_a, Hanna et al. (1982) suggests, in relation to Equation (16), replacing T_{s0} with T_{s0}/μ_s and T_{a0} with T_{a0}/μ_a.

The resulting equation of the plume centerline trajectory $\Delta h(t)$ is (Briggs, 1975)

$$\Delta h(t) = \left(\frac{3}{\beta^2} \frac{F_m}{u_0} t + \frac{3}{2\beta^2} \frac{F_b}{u_0} t^2 \right)^{1/3} \tag{20}$$

Equation (20) takes into account both the buoyancy and initial vertical momentum contributions. In the very initial stage, the momentum dominates and the plume rise is described by

$$\Delta h(t) = \left(\frac{3}{\beta^2} \frac{F_m}{u_0} t \right)^{1/3} \tag{21}$$

whereas, when t is larger than $2F_m/F_b$ (about 10 s for many sources, Briggs 1975) the buoyancy dominates and Equation (20) reduces to

$$\Delta h(t) = \left(\frac{3}{2\beta^2} \frac{F_b}{u_0} \right)^{1/3} t^{2/3} \tag{22}$$

Expressed as a function of downwind distance, Equations (20), (21) and (22) become

$$\Delta h(x) = \left(\frac{3}{\beta^2} \frac{F_m x}{u_0^2} + \frac{3}{2\beta^2} \frac{F_b x^2}{u_0^3} \right)^{1/3} \tag{23}$$

$$\Delta h(x) = \left(\frac{3}{\beta^2}\right)^{1/3} F_m^{1/3} x^{1/3} u_0^{-2/3} \tag{24}$$

and

$$\Delta h(x) = \left(\frac{3}{2\beta^2}\right)^{1/3} F_b^{1/3} x^{2/3} u_0^{-1} \tag{25}$$

In order to use the above equations in practical models, the value of β, the dimensionless entrainment parameter, must be empirically established. In the bent over buoyant plumes ($\phi \to 0$, where ϕ is the angle between the horizontal and the centerline) β = 0.6, whereas for vertical buoyant plumes ($\phi \to 90^0$) β = 0.11 (Briggs, 1975; Hoult and Weil, 1972). For jet plumes (Briggs, 1975, 1984)

$$\beta = 0.4 + 1.2\frac{u_0}{v_{s0}} \tag{26}$$

In particular, Equation (25) becomes

$$\Delta h(x) = 1.6 F_b^{1/3} x^{2/3} u_0^{-1} \tag{27}$$

This equation is widely known as the "two-thirds" law. It was confirmed by a large amount of experimental work (see Briggs, 1975 for a comprehensive summary). Figure 4 is an example of the quality of the agreement found in the literature. Consequently, most practical models use the "two-thirds" law to describe the plume rise in the transitional phase under neutral and unstable conditions. However some models - see, for instance, AERMOD (U.S. EPA, 1998) or Weil et al. (1997) - use the complete Equation (20). In this case they use the value β = 0.6 for the momentum term too.

By defining the momentum length scale L_m and the buoyancy length scale L_b as

$$L_m = \frac{\sqrt{F_m}}{u_0} \quad \text{and} \quad L_b = \frac{F_b}{u_0^3} \tag{28}$$

Equations (23 - 25) become

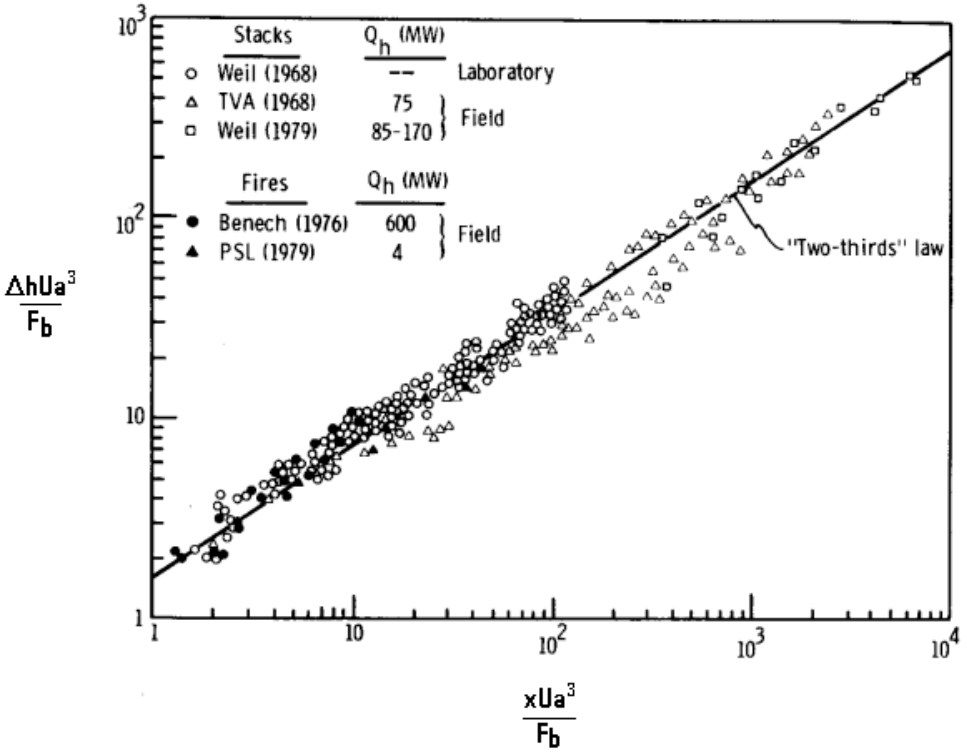

Figure 4. Observed trajectories of buoyancy-dominated plumes compared with the "two-thirds" law (from Weil, 1988). [Reprinted with permission from American Meteorological Society].

$$\frac{\Delta h(x)}{L_b} = \left[\frac{3}{\beta^2} \left(\frac{L_m}{L_b} \right)^2 \frac{x}{L_b} + \frac{3}{2\beta^2} \left(\frac{x}{L_b} \right)^2 \right]^{1/3} \tag{29}$$

$$\frac{\Delta h(x)}{L_m} = \left(\frac{3}{\beta^2} \frac{x}{L_m} \right)^{1/3} \tag{30}$$

$$\frac{\Delta h(x)}{L_b} = \left(\frac{3}{2\beta^2} \frac{x^2}{L_b^2} \right)^{1/3} \tag{31}$$

L_m and L_b allow an alternative criterion to establish in which range of downwind distances the buoyancy or the momentum dominates the plume rise: momentum dominates for $x << L_m^2 / L_b$ whereas buoyancy dominates for $x >> L_m^2 / L_b$.

2.2.2 Stable Case

In case of a stable atmosphere (s = const, $s \neq 0$), again neglecting ambient turbulence, and considering uniform wind and the bent-over phase, integration of the conservation equations leads to the following expression (Briggs, 1975)

$$\Delta h(x) = \left(\frac{3(1+k_v)}{\beta^2 u_0 s} \right)^{1/3} \left\{ N' F_m \sin\left(N' \frac{x}{u_0} \right) + F_b \left[1 - \cos\left(N' \frac{x}{u_0} \right) \right] \right\}^{1/3} \tag{32}$$

for $x \leq \pi u_0 / N'$, where $N' = s^{1/2} / (1+k_v)^{1/2}$. The term, $1+k_v$, accounts for the so-called "added mass" (Briggs, 1972, 1975, 1984; Weil, 1988, 1994). This added mass takes into account the momentum of the ambient air displaced by the rising plume. Consequently, the effective plume radius is larger than the visible plume radius. Many models did not consider this aspect that can explain the difference found in the value of the entrainment parameter from the measurements of plume rise in different stability conditions. Concerning the numerical value of the added mass, Briggs (1975) and Weil (1994) suggest $1+k_v = 2.25$.

When the atmosphere is stable, ambient turbulence is very low and a plume levels off where its density difference with respect to ambient air approaches zero. For distances greater than $\pi u_0 / N'$ a plume, in principle, overshoots its equilibrium height and displays a quickly damped oscillation. This was experimentally verified in some occasions (Briggs, 1975). However, often plumes approach an asymptotic height with no overshoot at all (Briggs, 1984). In this range of distances a plume drifts downwind with a very small increase in thickness, due to its mixing with stable, almost non turbulent, air.

In the two asymptotic cases in which the momentum dominates ($F_b << N' F_m$) or the buoyancy dominates ($F_b >> N' F_m$), the above equation reduces to, respectively

$$\Delta h(x) = \left[\frac{3(1+k_v)^{1/2} F_m \sin\left(N' \frac{x}{u_0} \right)}{\beta^2 u_0 s^{1/2}} \right]^{1/3} \tag{33}$$

$$\Delta h(x) = \left\{ \frac{3(1+k_v)F_b\left[1-\cos\left(N'\frac{x}{u_0}\right)\right]}{\beta^2 u_0 s} \right\}^{1/3} \tag{34}$$

Notice that, by approximating $\cos\left(N'\frac{x}{u_0}\right)$ as $1-\left(N'\frac{x}{u_0}\right)^2$ for $\frac{x}{u_0} << \frac{1}{N'}$ in Equation (32), the "two third law" - Equation (27) - is recovered.

2.3 Formulae for the Final Height of Buoyant Plumes

Stable stratification is the only condition in which a plume levels off and, consequently, the definition of a final height is correct. Since in neutral and unstable conditions the buoyancy flux F_b is conserved, plumes cannot, in principle, level off. However, ambient turbulence significantly affects the buoyant plume growth. Another limitation to the continuous rise of the plume is the presence, above the mixing height, of a capping inversion (see Section 5.2).

The importance of assessing correct ways to determine the plume "final height" derives from the wide use of Gaussian models in dispersion calculations. These dispersion models disregard the transitional phase and assume that a plume is emitted by a virtual height (see Figure 2) located at a final effective height h_e, given by the sum of stack height z_s and plume final rise Δh - see Equation (1).

2.3.1 Neutral and Unstable Case

For neutral or unstable conditions, Briggs (1969) suggested using Equation (27) up to $x = x_c^*$, and the following equation

$$\Delta h(x) = 1.6\, F_b^{1/3} u_0^{-1} \left(x_c^*\right)^{2/3} \left[\frac{2}{5} + \frac{16x}{25x_c^*} + \frac{11}{5}\left(\frac{x}{x_c^*}\right)^2\right]\left(1+\frac{4x}{5x_c^*}\right)^{-2} \tag{35}$$

for $x > x_c^*$. x_c^* is a critical distance representing the downwind distance at which ambient turbulence begins to dominate the entrainment process, which can be expressed either by

$$x_c^* = A_1 F_b^{2/5} z_s^{3/5} \qquad z_s < 305m$$

$$x_c^* = A_2 F_b^{2/5} \qquad z_s > 305m \tag{36}$$

or

$$x_c^* = A_3 F_b^{5/8} \qquad F_b < 55\, m^4/s^{-3}$$

$$x_c^* = A_4 F_b^{2/5} \qquad F_b > 55\, m^4/s^{-3} \tag{37}$$

in which the values of the four dimensional constants are the following: $A_1 = 2.16\, s^{6/5} m^{-6/5}$, $A_2 = 67.0\, s^{6/5} m^{-3/5}$, $A_3 = 49.0\, s^{15/8} m^{-3/2}$, and $A_4 = 119.0\, s^{6/5} m^{-3/5}$.

In the case of fossil fuel plants with Q_h of 20 MW or more, x_c^* can be satisfactory approximated by the following equation

$$x_c^* = 10 z_s \tag{38}$$

Subsequently, Briggs (1975) made a distinction between neutral and unstable conditions accounting for the effects of ambient turbulence on the plume rise. While self-generated turbulence affects the entrainment process near the source, ambient turbulence (with both small and large scale eddies) becomes important further downwind. Small scale eddies (with typical length scale $\leq R$), are responsible for the increase of the plume growth rate beyond that given by self-induced turbulence. The breakup model (Briggs, 1984; Weil, 1988), assumes that plume rise finishes when ambient turbulence "breaks up" the self-generated structure of the plume, causing a vigorous mixing and, consequently, plume gradually loses buoyancy and momentum and eventually level off. Thus, this process leads to an asymptotic rise. According to Briggs, the plume breakup occurs when the ambient rate of dissipation of turbulent kinetic energy, ε_a, exceeds the one of the plume ε_p. Large scale eddies (updrafts and downdrafts in the CBL) may transport plume segments up and down, thereby dispersing the plume by vertical meandering and pushing some of them to the surface. When this happens, the time averaged ground level concentration is more dependent on how many times, during the averaging period, the plume touches the ground than on the height of the asymptotic rise. As a consequence, in the CBL case the surface sensible heat flux, which plays the major role in the development of updrafts and downdrafts is assumed to be the leading parameter.

Therefore, for neutral conditions, in which the rise is limited by the mechanical ambient turbulence, Briggs proposed the iterative formula

$$\Delta h = 1.2 \left(\frac{F_b}{u_0\, u_*^2} \right)^{3/5} (z_s + \Delta h)^{2/5} \tag{39}$$

where u_* is the friction velocity. For unstable conditions, in which the termination of the rise is due to the breakup by plume-scale, Briggs (1975, 1984) proposed

$$\Delta h = 3.0\left(\frac{F_b}{u_0}\right)^{3/5} H^{-2/5} \tag{40}$$

where H is the upward surface sensible heat flux times $g/(c_p \rho_a \vartheta)$. This equation may be also written as

$$\Delta h = 3.0 F_*^{3/5} h \tag{41}$$

where

$$F_* = F_b/(u_0 w_*^2 h) \tag{42}$$

is the dimensionless buoyancy flux, w_* is the convective velocity scale and h is the mixing height. Notice that Hurley and Physick (1993) derived an expression similar to (41), but with the constant equal to 2 instead of 3. Examining the Willis and Deardorff (1983) CBL water tank experiment, they also found that a value of 2 gave better agreement than the value 3. Best et al. (1990, reference from Hurley and Physick, 1993), found 2.3 by fitting field ground level concentration (g.l.c.) data. It is difficult to decide which constant value is to be preferred due to the lack of direct measurements of the final height in this conditions and to the large scatter in the indirect methods (g.l.c.).

2.3.2 Stable Case

Let us consider Equation (32). This equation has its maximum, $\Delta h_{\max}$, for $x_f = \pi u_0 / N'$. Considering that for most hot plumes the effect of the initial momentum can be neglected, and that the leveling off or equilibrium height is observed to occur at about 5/6 $\Delta h_{\max}$, the following expression for the final height in stable and windy conditions $(u_0 > 1 \text{ ms}^{-1})$ is obtained

$$\Delta h = 2.8 (F_b / u_0 s)^{1/3} \tag{43}$$

However, Briggs (1975; 1984) on the analysis of many field and laboratory observations, found that a slightly different numerical coefficient, 2.6, yielded the best fit to the observation. Consequently, Briggs recommended that the most accurate estimate of the plume final height in stable conditions is given by

$$\Delta h = 2.6 (F_b / u_0 s)^{1/3} \tag{44}$$

For stable and calm conditions ($u_0 < 1\,\mathrm{ms}^{-1}$), in which a plume rises nearly vertically, Briggs (1969), on the basis of previous work of Morton et al. (1956) and the examination of many field observations, proposed

$$\Delta h = 5.0\, F_b^{1/4} s^{-3/8} \tag{45}$$

Subsequently, Briggs (1984) proposed for the same conditions

$$\Delta h = 5.3\, F_b^{1/4} s^{-3/8} - 6 r_s \tag{46}$$

2.4 Formulae for Jet Plumes in the Transitional Phase

Also these formulae, as the ones for buoyant plumes, have a semi-empirical origin.

The formulae for the transitional phase of jet rise, in neutral/unstable or stable conditions, were already introduced, namely Equations (24) and (33), in which the entrainment parameter β was defined by Equation (26).

2.5 Formulae for the Final height of Jet Plumes

For neutral conditions Briggs (1969) previously suggested

$$\Delta h = \frac{3 v_s d_s}{u_0} \tag{47}$$

where d_s is the internal diameter of the stack outlet, and later (1975, 1984) suggested

$$\Delta h = \frac{0.9}{\beta}\left(\frac{F_m}{u_0\, u_*}\right)^{1/2} \tag{48}$$

For unstable conditions Briggs (1975) suggested

$$\Delta h = 2.3\left(\frac{F_m}{u_0}\right)^{3/7} H^{-1/7} \tag{49}$$

and, subsequently, Briggs (1984) suggested for the same conditions

$$\Delta h = \frac{1.3}{\beta^{6/7}}\left(\frac{F_m}{u_0\, w_*}\right)^{3/7} h^{1/7} \tag{50}$$

Also in Equations (48) and (50) β is defined by Equation (26).

Briggs (1969, 1975) suggested for stable and windy conditions $(u_0 > 1\,ms^{-1})$

$$\Delta h = 1.5\,(F_m\, u_0^{-1} s^{-1/2})^{1/3} \tag{51}$$

This is obtained from considering that Equation (33) attains its maximum $\Delta h_{\max}$ for $x_f = \pi u_0 / (2N')$ and that the equilibrium height occurs at about 2/3 $\Delta h_{\max}$.

For stable and calm conditions $(u_0 < 1\,ms^{-1})$, Briggs (1969, 1975) suggested, on the basis of a few observations, the following relationship

$$\Delta h = 4.0\,(F_m\, s^{-1})^{1/4} \tag{52}$$

Taking into account that observations on the rise of jet plumes in stable conditions are very sparse, Briggs suggests considering the above formulae as tentative.

2.6 Buoyant Plumes or Jet Plumes

While for jets plumes or for highly buoyant plumes it is clear which type of plume rise formulae is to be used in practical dispersion applications, for cases in which $\Delta T_0 = T_{s0} - T_{a0}$ (where ΔT_0 is the temperature difference between emission and ambient air at the stack mouth) is greater than zero but not very high, whether the plume rise is dominated by momentum or by buoyancy must be determined. Two methods able to solve this problems are presented. The first one - see, for instance, AERMOD (U.S. EPA, 1998) - consists in using Equation (23) or (32) for the transitional phase in neutral/unstable or stable case, respectively. These cited equations include both contributions. The final plume height is calculated according to the methods resumed in Section 2.3.

The second one is based on the U.S. EPA models PTPLU (Pierce et al., 1982), SCREEN3 (U.S. EPA, 1995a), and ISC3 model (U.S. EPA, 1995b). In this method a critical temperature difference ΔT_c is defined. If $\Delta T_0 > \Delta T_c$ the plume has to be treated as buoyant; otherwise the plume has to be treated as a jet. ΔT_c is defined as:

- in stable atmosphere

$$\Delta T_c = 0.19\, v_{s0} T_{a0} s^{1/2} g^{-1} \tag{53}$$

- in neutral or unstable atmosphere

$$\Delta T_c = \begin{cases} 0.29\, v_{s0}^{1/3} T_{s0} d_s^{-2/3} g^{-1} & if\ F_b < 55\ m^4 s^{-3} \\ 0.056\, v_{s0}^{2/3} T_{s0} d_s^{-1/3} g^{-1} & if\ F_b \geq 55\ m^4 s^{-3} \end{cases} \quad (54)$$

The units of the two dimensional coefficients in Equation (54) are $m^{4/3}s^{-5/3}$ and $m^{2/3}s^{-4/3}$ respectively. Equation (53) is obtained by equating Equations (44) and (51) and solving for ΔT_0. Similarly, Equations (54) are obtained by inserting Equations (37) into (27) and then equating Equation (47).

2.7 Moore's and Netterville's Models for the Plume Rise of Buoyant Plumes

The formulae for the buoyant plume rise presented in the previous part of this Section form a complete and validated set of equations, widely used by the modeler community. However we briefly introduce also the Moore and Netterville models because we think that these two models are important for scientific and/or historical reason. As such, they may be of interest for the reader. Moreover, Netterville's parameterization of ambient turbulence is used later in the chapter (see Sections 3.2 and 4.4).

2.7.1 The Moore Model

Briggs models are, as we have seen above, derived by assuming that a plume is continuous, accounts for the crosswind and vertical spread and disregards the along wind spread and its diameter increases as it rises and travels downwind. For this reason this kind of approach is called “two-dimensional”. Instead Moore, (1974) points out that the dilution of an hot smoke plume is a three-dimensional phenomenon, because the plume, rather than rising as a continuous cone, breaks up into a discrete series of puffs which tend to recombine and merge into each other as the plume travels downwind, so that the number of puffs per unit length of plume decreases with downwind distance. The problem becomes three-dimensional because the along wind spread must be considered as well. One of the main interest in the Moore's model is in the recognition that observations of stack plumes sometimes reveal some three-dimensional features (Ooms, 1972) either due to its dynamic (formation of two counter-rotating vortices as it leaves the stack which may cause the plume bifurcation, split of the plume in lumps) or to terrain characteristics in case of low emissions.

Moore model is a generalized one that can be applied in a large variety of meteorological situations both during the transitional and final stage of rise without switching to various different expressions.

The basic difference between the two-dimensional and the three-dimensional approach is that in the former the plume rise is proportional to $F_b^{1/3}$, that is to $Q_h^{1/3}$, see Equations (9) and (27), whereas in the latter it results proportional to $Q_h^{1/4}$, namely

$$\Delta h(x) = A Q_h^{1/4} x_*^{3/4} u_{1.5}^{-1} \tag{55}$$

where: $u_{1.5}$ is the wind speed at the height $1.5\, z_s$; $x_* = x$ for short distances and $x_* = x_T$ for large distances. These two asymptotic values are connected by a smooth curve possessing the correct asymptotic and near field limiting forms:

$$x_* = \frac{x_T x}{\sqrt{x_T^2 + x^2}} \tag{56}$$

and x_T is given by the following expression

$$x_T = \frac{(D_0 + D_1 H^*) u_{1.5}}{\sqrt{(D_0 + D_1 H^*)^2 \dfrac{\Delta \vartheta^*}{D_2^2} + u_{1.5}^2}} \tag{57}$$

A, D_0 and *D_2* are dimensional constant, whereas *D_1* is dimensionless. Their values were estimated by Moore to be: A = 2.4 $MW^{-1/4} m^{5/4} s^{-1}$ for $z_s > 120$ m while, for $z_s < 120$ m, A = 2.4 for very stable conditions (i.e. for $\dfrac{\partial \vartheta / \partial z}{u_{1.5}^2} > 2.5$ K s^{2}m^{-3}), otherwise $A = 2.4(0.16 + 0.007 z_s)$; D_0 = 1920 *m*, D_1 = 19.2, and D_2 = 120 *ms*. H^* and $\Delta \vartheta^*$ are parameters related, respectively, to the following two assumptions: 1) the atmospheric turbulence effects on the first steps of the plume rise evolution are dependent on the height for low sources ($z_s < 120$ m), but independent of the height for high sources ($z_s > 120$ m); this assumption is parameterized setting: $H^* = z_s$ if $z_s < 120$ m, $H^* = 120$ m if $z_s > 120$ m; 2) the atmosphere is assumed to be stably stratified, even in convective conditions; since $\Delta \vartheta_{100}$ is the variation in potential temperature per each 100 m of height increase, this assumption is parameterized setting: $\Delta \vartheta^* = 0.08$ K if $\Delta \vartheta_{100} < 0.08$K, $\Delta \vartheta^* = \Delta \vartheta_{100}$ if $\Delta \vartheta_{100} > 0.08$K.

Moore claimed that his model is applicable when the difference in temperature between effluent and air ranges between 80 and 150 K, the effluent emission velocity v_{s0} does not considerably overtake the value of 30 m s^{-1} and in the following conditions: $x > 400$ m; $30\text{m} < z_s < 230\text{m}$; $10\text{ MW} < Q_h < 150\text{ MW}$.

An explicit expression of the final height is obtained by inserting $x_* = x_T / \sqrt{2}$ in Equation (55).

2.7.2 The Netterville Model

Netterville (1990) gave a detailed description of the entrainment process, which he called the "two-way model". This is based on an understanding of several quantitative aspects of turbulent mixing within free shear layers and on the availability of more detailed ambient turbulence data from remote sensors, like SODARS and RASS.

The two-way entrainment model predicts that the turbulent atmosphere must entrain plume material just as the plume must entrain the atmosphere. Figure 5 (from Netterville, 1990) illustrates what is meant with two-way entrainment. It shows a turbulent plume of radius R that rises at relative speed W through an atmosphere containing turbulent eddies of length scale r_a and relative root-mean-square velocity v'_a. The plume cross-section is assumed to have a 'spongy' internal structure caused by atmospheric turbulence eddies, in transit through the plume, that form transient holes in the surrounding matrix of turbulent plume material. Similarly, also the ambient air eddies become spongy due to penetration by the plume's internal turbulent eddies.

The entrainment process is split into three processes: direct entrainment (a process by which plume eddies, due the self-generated turbulence, capture ambient air masses), indirect entrainment (ambient air eddies in the plume that are in turn penetrated by eddies of the internal plume) and extrainment (transfer of plume mass from the plume itself to ambient air due to the turbulent eddies that enter the plume and carry off plume mass).

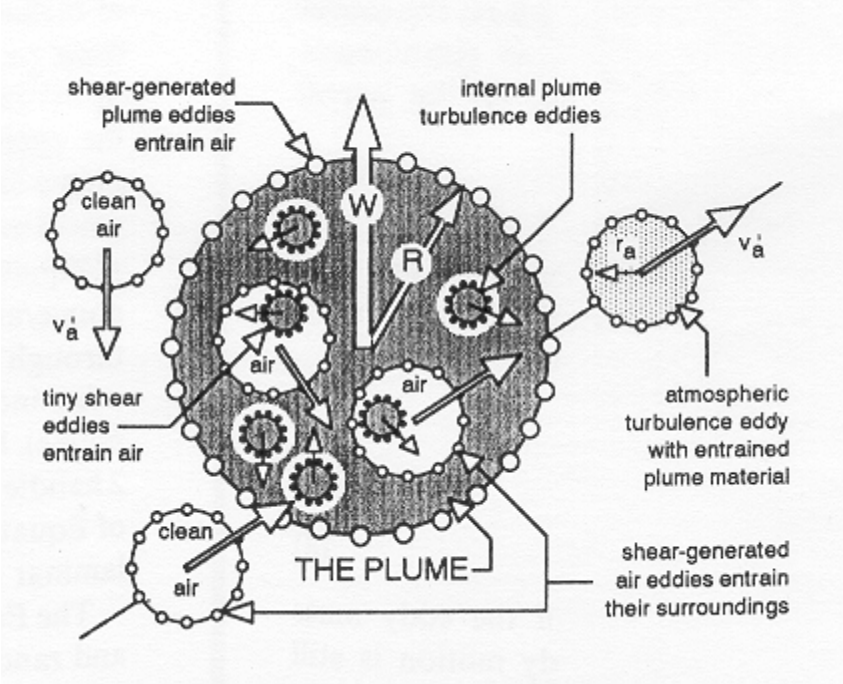

Figure 5. Schematic of plume/atmospheric interaction (from Netterville, 1990). [Reprinted with permission from Elsevier Science]

Netterville plume rise model is based on this description of entrainment process, and on the solution of the mass, momentum and energy conservation equations. The same simplifying assumptions on the plume shape and atmospheric conditions as in the Briggs models are made, thus obtaining the following scheme.

In stable atmosphere ($N^2 > 0$)

$$\Delta h(\tau) = \left\{ \frac{3}{\beta^2 u\left(f_b^2 + s\right)} \left[F_e + f_b M_e + \left\{ N M_e \left[\sin\left(\frac{N}{f_b}\tau\right) - \frac{f_b}{N}\cos\left(\frac{N}{f_b}\tau\right) \right] + \right.\right.$$
$$\left.\left. - F_e \left[\cos\left(\frac{N}{f_b}\tau\right) + \frac{f_b}{N}\sin\left(\frac{N}{f_b}\tau\right) \right] \right\} \exp(-\tau) \left] + \left(\frac{R_e}{\beta}\right)^3 \right\}^{1/3} - \frac{R_e}{\beta} \tag{58}$$

where $\tau = t\, f_b$ is the dimensionless plume travel time given by the product of the plume travel time, *t*, and the atmospheric turbulence buffet frequency, f_b. This last is defined as

$$f_b = 2\beta\sigma_u / (u\,\tau_E) \tag{59}$$

in which τ_E is the Eulerian integral time scale of atmospheric turbulence and σ_u is the standard deviation of longitudinal horizontal wind.

In neutral atmosphere ($N^2 = 0$)

$$\Delta h(\tau) = \left\{ \frac{3}{\beta^2 f_b^2 u} \left[F_e + f_b M_e - \left\{ f_b M_e + F_e(\tau + 1) \right\} \exp(-\tau) \right] + \right. \\ \left. + \left(\frac{R_e}{\beta} \right)^3 \right\}^{1/3} - \frac{R_e}{\beta} \tag{60}$$

In unstable atmosphere ($N^2 < 0,\ N \equiv +\sqrt{|N^2|}$)

$$\Delta h(\tau) = \left\{ \frac{3}{\beta^2 u \left(f_b^2 + s \right)} \left[F_e + f_b M_e - \left\{ N F_m \left[\sinh\left(\frac{N}{f_b} \tau \right) - \frac{f_b}{N} \cosh\left(\frac{N}{f_b} \tau \right) \right] + \right. \right. \\ \left. \left. + F_e \left[\cosh\left(\frac{N}{f_b} \tau \right) + \frac{f_b}{N} \sinh\left(\frac{N}{f_b} \tau \right) \right] \right\} \exp(-\tau) \right] + \left(\frac{R_e}{\beta} \right)^3 \right\}^{1/3} - \frac{R_e}{\beta} \tag{61}$$

As $t \to \infty$, all three solutions asymptotically approach the same functional form for final rise

$$\Delta h = \left[\left(\frac{3}{\beta^2 u} \right) \frac{F_e + f_b M_e}{\left(f_b^2 + s \right)} + \left(\frac{R_e}{\beta} \right)^3 \right]^{1/3} - \frac{R_e}{\beta} \tag{62}$$

In the above equations, F_e, M_e, and R_e are initial values of plume buoyancy, momentum and radius at the end of bending-over phase. Djurfors (1983) has shown that they are given by

$$R_e \cong r_s \left(2 \frac{v_{s0}}{u} \frac{T_a}{T_{s0}} \right)^{1/2} \tag{63}$$

$$M_e = F_m \left(\frac{v_{s0}}{u} \frac{T_a}{T_{s0}} \right) \tag{64}$$

$$F_e = F_b \tag{65}$$

For stable conditions ($s > 0$) the final rise is always finite. For neutral conditions ($s = 0$) the final rise is finite only if the atmosphere is turbulent ($f_b > 0$). For unstable conditions ($s < 0$) the final rise is finite or infinite depending on the sign

of $\left(f_b^2 + s\right)$, i.e. on whether thermal instability or atmospheric turbulence dominates plume motion.

The Netterville plume rise model is consistent with the 'decay constant' approach of Djurfors (1977), which recognized that the mathematical form of leveling-off behavior was one in which the vertical distance between the plume centerline and its final height would decrease exponentially with time.

The validation of this model is based on one data set of LIDAR measurements.

3 Advanced Plume Rise Models

3.1 Introduction

The semi-empirical formulations presented in the previous section have shown, on several occasions, a great degree of uncertainty. This is partly due to the simplifications introduced in such formulations. Advanced methods, based on the numerical integration of a set of differential equations expressing the conservation equations and on revised entrainment assumptions, have been proposed. They account explicitly sufficient transport mechanisms to be of general use, particularly in the cases that are too complicated to be modeled by simple analytical models. They provide, at least in principle, a better physical representation of the two basic phenomena related to plume rise: the grow of the plume centerline and the entrainment of ambient air into the plume and its consequent horizontal and vertical spreading. They also allow dealing with complex atmospheric conditions. However, they require more computational resources and more detailed input data.

Among the advanced models we may distinguish: integral models (they use spatially integrated forms of the fluid motion equations), differential models (they integrate on Eulerian grids Reynolds-averaged flow conservation equations) and large eddy simulation (LES) models. In all these models, the system of equations must be closed by a proper number of assumptions and closure hypothesis. Essentially they are empirical, but are based on physical reasoning and/or observations.

The first two categories, that are not so computationally costly (particularly for nowadays computers) are not only of scientific interest, but may also be useful tools in air pollution modeling, since they are able to deal with any kind of stack plume (jet, dense or buoyant plume) and complex atmospheric structures.

We would like to stress the importance of initialization in numerically solving the plume rise equations. Stack geometries and plume exit temperatures and

velocities may vary over wide ranges. Consequently, large errors in the plume rise estimations can be made if the initial conditions are not correctly formulated.

Many advanced models have been developed. It is hopeless to review them all, therefore only some of them are briefly presented below. We would also mention that a number of the most recent advanced plume rise models are based on Lagrangian particle techniques. These last models for plume rise are discussed in Section 4.

3.2 Integral Models

The models developed by Schatzmann (1979), Ooms and Mahieu (1981), Glendening et al. (1984), Chiang and Sill (1985), Gangoiti et al. (1997) and Janicke and Janicke (2001) are considered here. They give an overview of these kind of models developed during the last 20 years. There are some characteristics common to all these models. Since the trajectory of a plume (jet, dense or buoyant) in windy conditions is not a straight line, they generally use the natural coordinate (or curvilinear) system that moves and rotates as it follows the plume centerline trajectory, rather than the Cartesian coordinate system. They do not use the common Boussinesq approximation thus allowing the treatment of plumes with greatly different density from that of ambient air. The plume is assumed to exhibit local similarity, i.e., the shapes of the radial profiles of excess velocity, temperature and concentration do not change downstream. The profiles of plume velocity, temperature, and density are assumed to be of Gaussian (Schatzmann, 1979; Ooms and Mahieu, 1981; Chiang and Sill, 1985), "top hat" (Glendening et al., 1984) or exponential (Gangoiti et al., 1997) shape for mathematical simplicity. Models do not use different parameterizations for each phase (buoyancy dominate, intermediate and turbulence dominated) of the plume trajectory. Additional assumptions are steady state conditions for both plume and environment, zero environmental vertical velocity and absence of stack downwash effects (see Section 5.1), which is appropriate for plumes with large buoyancy, and exit velocity. In most models it is assumed that the mean excess and turbulent quantities plume are axisymmetric and, consequently, that the three-dimensionality of the plume motion can be ignored. Although it is recognized that two counter rotating vortices are formed at the stack mouth exit and that the plume may break into distinct puffs (that may also merge downwind), these effects are neglected since they are assumed to be incorporated in some way in the entrainment formulations. All the models were tested against laboratory and field data.

Basically, the main difference among the various models lies in the modeling of entrainment, i.e. the rate of mixing of ambient air into the plume. Other characteristics that make different the models are the inclusion in some of them of pollutant dispersion besides the path and spread of the plume or the capability of some models to treat arbitrary atmospheric structures, whereas the others should divide the atmosphere in a certain number of layers with different constant

atmospheric properties. Only a few models accounts for the plume rise modifications due to the condensation of plume water vapor.
The plume rise model of Schatzmann (1979) assumes that the wind velocity is constant in value and direction and that the atmosphere is stratified with a constant density gradient. It includes seven equations for the following seven unknowns: centerline excess velocity, temperature and concentration, centerline density defect, jet radius, angle of inclination and local rate of entrainment. A rather complex entrainment function is used which is based on the local densimetric Froude number, the plume radius, the macroscale of the energy-containing eddies, angle of the plume trajectory, free-stream velocity, centerline excess velocity and five empirical constant. The tests of the model performances against many observations including jets, buoyant and dense plumes, gave reasonable agreement. This model, however, fails to account for the inertia of "effective mass" outside the plume, seems to contain an unrealistic drag term, and shows problems in the mass conservation equation (Briggs, personal communication to Zannetti, from Zannetti, 1990).

Ooms and Mahieu (1981) proposed a model able to calculate both the path of the plume in a windy atmosphere and the ground level concentration. Such model is a development of the method for the calculation of the plume path, therefore of the plume rise as well, presented in Ooms (1972) and Ooms et al. (1974). The model contains eight equations: two equations relate the Cartesian coordinate to the curvilinear coordinates; six equations describe the entrainment, conservation of mass (pollutant), momentum in the x-direction and in the z-direction and energy; the last equation expresses the assumed atmospheric linear stratification. The description of the entrainment and the drag force, is based on the theoretical work of Abraham (1970) and Loh-Nien Fan (1967). The rate of entrainment of air into the plume due to atmospheric turbulence depends on the eddy energy dissipation ε. For neutral conditions a relation for ε due to Briggs (1969) is used and for the other stability conditions data from Kaimal et al. (1976) are considered. Cross-sections of the plume are assumed to be ellipses. Moreover, this model takes into account the first part of the plume, known as the zone of flow establishment, and also the turbulence and stratification of the atmosphere so that the influence of the different stability on the plume path can, in principle, be studied. The simulated ground level concentrations were compared with those obtained by a classical Gaussian plume model (using Briggs formulae – see Section 2 – for plume rise and Singer-Smith, 1966, sigma curves). The agreement was good in neutral and unstable conditions, while large differences were found in stable conditions.

The Ooms and Mahieu model is used in the ADMS model (e.g., Carruthers et al., 1999).

The plume rise model proposed by Glendening et al. (1984) is able to treat arbitrary complex atmospheric structures also when there are large vertical variations in atmospheric stability or wind velocity (conditions particularly common for near shoreline power plants). The model consists of a set of eight

ordinary differential equations (conservation of mass, energy, horizontal x and y momentum, vertical momentum, plus three relationships between curvilinear and Cartesian coordinates) and three equations (gas equation and the definitions of virtual temperature and virtual potential temperature). Entrainment is parameterized according to Hewett et al. (1971). Profiles of temperature and wind are needed to run the model. The accuracy of the model prediction, verified against field observations, were found satisfactory and superior to those from a standard plume rise formula - Equation (44).

The Glendening et al. plume rise model, as modified by Hurley and Manins (1995), is used in the models LADM (e.g., Physick, 1996) and TAPM (e.g., Hurley et al., 2001; see also Section 4.3.2).

The model developed by Chiang and Sill (1985) is applicable to all stability conditions but only to simple atmospheric structures (that can be expressed by analytical relationships). The governing equations express the conservation of mass, momentum in the direction oriented along the plume path and to the normal to it, thermal energy and tracer concentration. Two relationships between natural and Cartesian coordinates are also used and the system is closed with an entrainment model. Basically, the authors' interest was to develop new entrainment models. Thus they proposed different entrainment models for different turbulent mixing mechanisms (such as shear, buoyancy, or ambient turbulence). Then, these authors proposed that, when the turbulent mixing is due to the contemporary action of different mechanisms, the total entrainment rate is the linear combination of the various rates derived individually from growth rate models, i.e. a superposition approach.

The agreement between predicted plume trajectories, velocities and dilution rates and the observed ones was satisfactory.

Gangoiti et al. (1997) presented a three-dimensional plume rise model for tall stacks capable of dealing with complex atmospheric profiles. Ambient turbulence is assumed to be homogeneous and isotropic, the plume is considered to exit from the stack as a mixture of dry combustion gas, water vapor and liquid water. Dry air and ambient water vapor, but not liquid water, are then entrained during the plume motion. Thus the model allows for condensation and/or re-evaporation within the plume. Condensation in a moist atmosphere increases buoyancy through release of latent heat while evaporation of droplets absorbs latent heat from the plume, which consequently loses buoyancy. The classical parameterization for entrainment of air into plume due to the self-generated turbulence has been completed with entrainment-extrainment processes in turbulent winds. This is based on the model of turbulent mass transfer between plume and environment proposed by Netterville (1990, see Section 2.7). A set of equations describing in great details the balance of mass, momentum and energy in the plume constitutes the model. This can be used also to predict plume penetration into elevated inversion layers but can provide only qualitative

estimates of the fraction of plume material that penetrates into them (see Section 5.2).

These authors compared the performance of their numerical model with a set of simpler models widely used in regulatory applications for plume rise calculation. Plume condensation has been found to be a major cause of underestimation in those simpler models, while wind shear causes systematic overestimation in stably stratified atmospheres. The assumed power law similarity profiles for the plume temperature and velocity gave better results in light winds (< 1.5 ms^{-1}) than the "top hat" profiles.

Also the PLURIS model (Janicke and Janicke, 2001) can be applied to situations with arbitrary three-dimensional wind fields and to both dry and moist plumes. Arbitrary directions of the source exit can be considered. Unlike models based on a similarity profile description, it is not necessary to make assumptions about the structure or symmetry of the plume cross-section or about the zone of flow establishment near the source exit. The similarity profiles enter into the model only via the definition of the liquid water content and affect mainly the prediction of the visible plume boundary. In the absence of condensation, the model is independent of any similarity profile assumptions. The model consists of 8 differential equations for mass, *x, y, z*-momentum, enthalpy, velocity fluctuations, total water content, and concentration. In addition, there are three differential equations for the three Cartesian coordinates of the plume axis. In the special case of a bent-over plume the model can be solved analytically. The model was validated by a direct comparison with various plume rise measurements obtained by means of water tank, wind tunnel, and field experiments. The model is presently implemented and used in combination with the Lagrangian dispersion model LASAT (Janicke, 1983).

3.3 Differential Models

Golay (1982) proposed a differential entrainment model. It is able to simulate bent-over plumes in complex vertical atmospheric structures by numerically integrating the conservation equations of mass, momentum, heat, water vapor, liquid water, and the two equations for the turbulent kinetic energy and eddy viscosity in a form presented by Stuhmiller (1974). It uses a mixed Eulerian-Lagrangian reference system. A two-dimensional Eulerian computational mesh translates downwind at a plume mass averaged wind speed.

Data from field study of airborne SO_2 plume and for ground level SO_2 concentration were used to test the model performances. The model simulations resulted in better agreement with observations than those obtained by standard analytical formulations.

The major limitation of Golay's approach is the detailed meteorological information that is required; i.e., the vertical profiles of wind speed, virtual

potential temperature, relative humidity, turbulent kinetic energy, and turbulent viscosity.

3.4 LES Models

Probably the most promising technique for the simulation of buoyant plumes in unstable conditions, at least from a theoretical viewpoint, is the Large Eddy Simulation (LES). These model simulations allow studying in great details the contribution to the plume motion caused by convective turbulence and that caused by plume buoyancy. Nieuwstadt and de Valk (1987) applied such a model to a line source, in which buoyancy was added by increasing the temperature of the source with respect to the ambient temperature. Then they solved the equation for the concentration conservation simultaneously with the other LES equations. Further work in this direction was performed by van Haren and Nieuwstadt (1989), who obtained reasonable agreement between the output of their LES, which however considered only a modest plume buoyancy, and the field experiments of Carras and Williams (1984). It was found that the fraction of the plume motion caused by plume buoyancy does not seem to obey the "two-thirds" law. Plume buoyancy strongly affects the contribution of ambient turbulence to the mean plume height. Nieuwstadt (1992a) showed that the two contributions (internal buoyancy and ambient turbulence) cannot simply be calculated independently but that they interact. Thus ambient convection influences the plume rise (large eddies modify the entrainment) and vice versa (the interaction ambient turbulence – plume motion depends on plume rise which transports the plume to different PBL heights).

Zhang and Ghoniem (1993, 1994 a,b) developed a computational model based on the Lagrangian interpretation of the dynamics of buoyancy-driven flows that uses the vortex element and transport element methods to solve the governing equations. The solution they have constructed causes the model to be considered as a LES model, since the governing equations describe the effects on the plume motions of the large scales and the small scales are modeled phenomenologically (Zhang and Ghoniem, 1993). They faced problems of increasing complexity in three subsequent papers: firstly they considered a neutral atmosphere with small scale turbulence in a horizontal uniform wind (Zhang and Ghoniem, 1993), then considered a linearly stratified atmosphere (Zhang and Ghoniem, 1994 a) and, finally, a linearly stratified atmosphere capped by an inversion layer (Zhang and Ghoniem, 1994 b). The following results may be important not only from a theoretical point of view but also for their practical implications. In neutral atmosphere it was found that the plume cross-section is kidney-shaped and that the initial shape of the cross-section (that can be circular or elliptical) has some effects on the plume trajectory. In the case of a circular plume the "two-third" law is closely followed. The entrainment is dominated by large scale engulfment which is inhomogeneous and non-isotropic. In the second case, linearly stratified atmosphere, it was found that the entrainment constant β (estimated equal to 0.49) mainly affects the equilibrium height, whereas the added mass constant k_v

(see Section 2.2.2 – estimated equal to 0.7) influences the downwind distance where this equilibrium height is reached. In the third case, the interaction of the plume with an inversion layer (i.e.: partial or total or null plume penetration - see also Section 5.2) has been studied. In particular it was found that when the plume bumps against an inversion layer, internal gravity waves are generated along the layer, radiating the energy of the plume and reducing its penetration capacity.

4 Particle Models for Plume Rise

4.1 Introduction

In Eulerian and Gaussian models, the final plume height Δh is generally computed by means of simple analytical expressions (like those presented in Section 2 of this chapter) and inserted in the model as an input parameter. On the contrary the inclusion of plume rise in Lagrangian Stochastic Models (LSM, see also Chapter 11) can be done dynamically, i.e. each particle, at each time step, can be acted upon by local wind speed and direction, ambient stability and turbulence (both the self-generated and ambient ones). Therefore it is possible to obtain a degree of resolution and accuracy not obtainable with other simulation techniques. Furthermore, the interaction of a plume with a capping inversion layer can be simulated in a rather "natural" way. However the correct incorporation of plume rise in LSM is still an open problem, since it is needed to simulate the entrainment phenomenon, that is the exchange processes between the plume particles and the turbulent environment must be described. Since entrainment acts, primarily, at the edge of a plume, the position, velocity and buoyancy of the other particles should be also taken into account.

A completely satisfying approach, based on fundamental particle behavior, is not yet available. Nevertheless many formulations have been proposed in the literature to practically solve the problem, with a different degree of approximation, allowing the plume rise calculation in LSM. They try to achieve a good compromise among computational requirements, physical consistency and reliability of the numerical results. Indeed, most of them proved to give reliable results when compared to laboratory and/or field data. In the following these approaches will be presented. They include: empirical methods; semi-empirical methods, in which the plume rise is computed by numerically integrating, at each time step, the conservation equations - see Equations (2 - 5) - and the plume spread is calculated by the Langevin equation for the vertical velocity; theoretical models, in which an attempt is made of directly simulating the rise of buoyant plumes in a Lagrangian framework.

4.2 Empirical Methods

The first attempt to include plume rise into LSMs, taking into account the vertical variation of wind and stability, was done by Zannetti and Al-Madani (1984). Let

us recall (see Chapter 11) that in LSMs, the vertical particle positions X_z is generally computed, at each time step Δt, as follows

$$X_z(t+\Delta t) = X_z(t) + [U_z(t) + w'(t)]\Delta t \tag{66}$$

where $U_z(t)$ represents the mean vertical wind component (generally equal to zero in flat terrain) and $w'(t)$ refers to the ambient turbulent term (random forcing) which is computed from a stochastic equation for the velocity fluctuation. The idea, is to add an additional vertical velocity accounting for the buoyant rise, w_b, to Equation (66), thus obtaining

$$X_z(t+\Delta t) = X_z(t) + [U_z(t) + w'(t) + w_b]\Delta t \tag{67}$$

They expressed this extra-velocity by time differentiating an empirical analytical plume rise equation for the transitional phase (TVA formula – Strom, 1976). The same plume rise contribution is given to all the particles provided they are at the same height and have the same age. The plume spreads in the vertical as a consequence of the ambient turbulence only. This last appears in the stochastic equation for the vertical velocity. This method can correctly simulate the ensemble averaged plume mean height (provided the used analytical formula is correct), but the vertical spread, particularly in convective conditions, is likely to be underestimated. The authors presented some numerical examples showing how the method works and its ability to give qualitatively reasonable results. However they did not indicate how to compute the time at which the plume rise stops contributing to the vertical particle motion. They also suggested a possible alternative method that could better simulate the vertical spread, but without developing it. It consisted in tagging each particle with a random buoyancy of "suitable intensity".

Cogan (1985) was the first to try to model the entrainment process, even if on an empirical basis. The plume is divided into layers of constant thickness and, within each layer, it is separated into an inner region (containing the particles included within the center of mass $\pm$ one standard deviation) and an outer region. In the inner region the temperature of each particle is computed as a function of its distance from the center of mass, whereas in the outer region the particle temperature is reduced by a preset amount. This last depends on the chosen value of the entrainment constant.

Shimanuki and Nomura (1991) tried to numerically simulate the instantaneous images of chimney plumes under convective conditions. Their technique is based on single Lagrangian particle trajectories, whose velocity fluctuations are spatially correlated. The spatial auto-correlation function is prescribed in a completely empiric way and all the trajectories within a single cell assume the same value of the spatial auto-correlation function. The buoyancy effect is roughly accounted for by assigning a given initial vertical velocity to each

particle. The air stability does not affect directly the particle motion but is taken into consideration in the computation of turbulence scales.

The Zannetti and Al-Madani (1984) suggestion was applied by Anfossi et al. (1993) for buoyant plumes and by Anfossi (2000) for jet plumes. To each i-th particle a normally distributed buoyancy flux F_b^i is assigned at the stack exit, fixing the mean value equal to the mean buoyancy flux $\overline{F_b}$ and the standard deviation equal to $\overline{F_b}/3$ (this value, 1/3, was empirically fixed requiring that the plume radius near the source was approximately equal to $0.6\Delta h(z)$). In the case of a jet plume, F_m^i, $\overline{F_m}$ and $\overline{F_m}/3$ are used. Instead of computing w_b by means of an empirical analytical plume rise equation for the transitional phase only, they assumed that the plume centerline grows according to a plume rise formula describing both the transitional and final phases and different stability conditions. Thus, a simple algebraic expression giving a smooth curve and possessing the correct asymptotic and near field limiting forms was used. This interpolation curve was built following the Moore's suggestion - see Equation (56). For buoyant plumes, the interpolation curve has the following expression (Anfossi, 1985)

$$\Delta h(t) = 2.6\left(\overline{F_b}\, t^2 / U_a\right)^{1/3}\left(t^2 s + 4.3\right)^{-1/3} \tag{68}$$

and was obtained considering the “two-thirds” law - Equation (27) - for the transitional phase both in neutral/unstable and stable conditions (Arya, 1999) and Equations (44) for the final rise in stable conditions. For neutral/unstable conditions (s = 0) the plume final height is fixed according to Equation (38). The low wind speed conditions are dealt with inserting a minimum wind speed (0.3 ms^{1}). w_b is computed as follows

$$w_b = \frac{\Delta z}{\Delta t} = \frac{\left[\Delta h(U_a, s, t+\Delta t) - \Delta h(U_a, s, t)\right]}{\Delta t} \tag{69}$$

The model simulations were validated against DIAL measurements of a Thermal Power Plant plume in complex terrain (Anfossi et al., 1993). Predicted plume centerline height and horizontal and vertical plume width satisfactorily compared to the observed ones.

This method is used in the 3-D Lagrangian Stochastic Model SPRAY (Tinarelli et al., 2000; Finardi et al., 2001), which is also used (in some complex terrain cases) for regulatory purposes in Italy.

Equation (68) was also used by Graziani et al. (1997) for their LSM simulation of the dispersion of the volcanic emission from Vulcano Island.

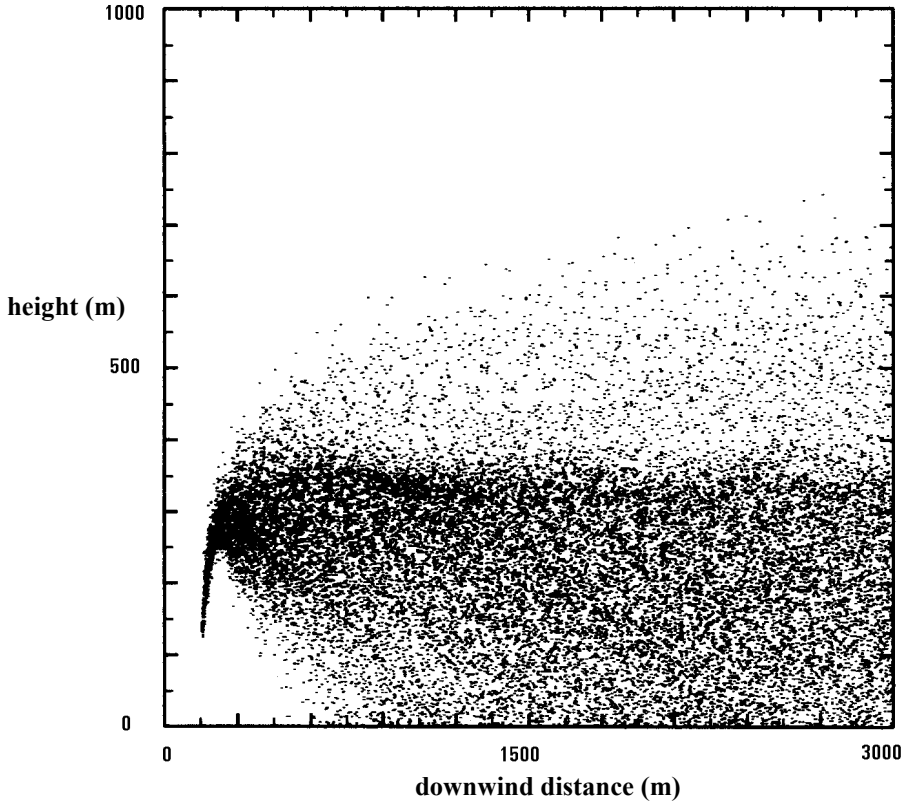

Figure 6. See the text (adapted from Anfossi et al., 1993). [Reprinted with permission from Elsevier Science].

Figure 6 shows a simulation result of this approach in non-homogeneous vertical meteorological conditions, in which simpler analytical approaches cannot be used. It refers to a typical fog situation in the Po Valley (Northern Italy): the fog layer extends from ground level to 250 m, an inversion layer with a large temperature increase (8 °C) lies between 250 and 400 m and the superior layer is nearly isothermal. Nearly calm conditions prevail ($u_0 \cong 1 ms^{-1}$). Each point in Figure 6 represents a model particle position. One can see that the rise of the plume is stopped by the inversion layer, that the pollutant reaches the ground level very close to the stack (fumigation) and that a partial inversion penetration occurs.

The case of jet plume is similarly treated. The starting points are the Briggs' formulae for jet plumes, Equations (24), (48), (51), and (52). Equation (24) works in the transitional phase, where the other equations are valid for the final stage of rise both in neutral and stable windy or calm conditions. In this case, Equation (68) becomes:

- for neutral conditions

$$\Delta h(x) = d_1 F_m^{1/3} u_0^{-2/3} t^{1/3} \left[\left(\frac{d_1}{d_2} \right)^6 \frac{U_a^4 t^2}{F_m} + 1 \right]^{-1/6} \tag{70}$$

were: $d_1 = 2.3$ and $d_2 = \dfrac{0.9}{u_*^{1/2}\left(0.4 + 1.2 \dfrac{U_a}{v_s} \right)}$;

- for stable and windy conditions $(u > 1 \text{ m s}^{-1})$

$$\Delta h(x) = d_1 F_m^{1/3} U_a^{-2/3} t^{1/3} \left[\left(\frac{d_1}{d_3} \right)^6 s^2 t^2 + 1 \right]^{-1/6} \tag{71}$$

were: $d_3 = 1.5$;

- for stable and calm conditions $(u < 1 \text{ m s}^{-1})$

$$\Delta h(x) = d_1 F_m^{1/3} U_a^{-2/3} t^{1/3} \left[\left(\frac{d_1}{d_4} \right)^6 \frac{F_m^{1/2} s^{3/2} t^2}{U_a^2} + 1 \right]^{-1/6} \tag{72}$$

were: $d_4 = 4$.

The vertical velocity, w_m, is computed as in Equation (69) and the plume rise calculation is stopped when the difference between $\Delta h(x)$ and the corresponding asymptotic final value is less than a chosen small value.

Also Souto et al. (2001) estimated the rise of buoyant plumes according to Equation (67). The extra velocity due to the buoyancy effects, w_b, was estimated as follows

$$w_b = \frac{1.35 F^{1/3}}{\Delta t} \frac{x^{0.58}}{u} \tag{73}$$

in unstable conditions and

$$w_b = \frac{2.04}{\Delta t} \left[\frac{0.86 F \left(1 - \cos(Nx / U_a \right)}{N^2 U_a} + r_s^3 \right]^{1/3} \tag{74}$$

in stable conditions. The numerical coefficients of these equations and the x exponent in Equation (73) were obtained by best fit of field observations. Equation (74) was proposed by Zhang and Ghoniem (1994a). This plume rise

calculation was inserted in two operational models, a LSM and an adaptive puff model.

4.3 Semi-Empirical Methods

Some interesting methods for incorporating buoyancy effects in LSM, were proposed by Luhar and Britter (1992), Hurley and Physick (1993), Hurley (1999, 2000) - these two methods are inserted and operative in the CSIRO models LADM and TAPM - and Weil (1994). Instead of assuming valid an analytical formula (or an interpolation formula), these methods compute the mean plume rise by directly solving the energy, mass and momentum conservation equations. This procedure is time consuming. However, also the Langevin equation, computing the velocity fluctuations, is already numerically solved. Therefore the increase in calculating time, with present days computer technology, is likely not to be a real problem. Different schemes are used to compute the plume spread and the interaction of ambient turbulence with the plume.

4.3.1 The Luhar and Britter (1992) Method

The LSM of Luhar and Britter (1992) accounts for the effects of source buoyancy on plume dispersion in the CBL by including the mean plume rise and the additional dispersion due to plume's self-generated turbulence. To incorporate the mean plume rise they added a new acceleration term in the Langevin equation for the vertical velocity component of their previously developed LSM (Luhar and Britter, 1992) for the dispersion of passive plumes in the CBL (consequently, the model is one-dimensional). The new acceleration term was based on the following expression

$$g\frac{\left(\rho_a - \rho(t)\right)}{\rho_a} = -U_a \frac{dW}{dx} \tag{75}$$

where $\rho(t)$ is the plume density at travel time t (= x/U_a). In the model, it was assumed that in the CBL the effects of ambient stability and wind shear on plume dispersion and rise could be neglected since the potential temperature and horizontal wind do not change appreciably with the height. This assumption allowed using the conservation equations in a simplified form, valid in the neutral boundary layer. The solution obtained from these equations for the mean vertical velocity W for three phases of plume development was used in Equation (75). The three phases correspond to the three different entrainment relationships of Slawson and Csanady (1971). During the initial phase, the intermediate phase, and the final phase, plume's self-generated turbulence, inertial sub-range turbulence, and energy containing eddies, respectively, govern plume rise. The expression for W in the initial phase of the rise, for example, is

$$W = \left(\frac{4}{9\beta^2} \right)^{1/3} F_b^{1/3} x^{-1/3} \tag{76}$$

which corresponds to the well-known 'two-thirds' behavior of plume rise. Luhar and Britter (1992) emphasized the importance of including the ambient turbulence effects in calculating W through the use of the entrainment relationships of the last two phases. Effects of plume's initial momentum on plume rise were also included.

To account for the additional dispersion due to the self-generated turbulence, the model assumed that the mass, and hence the computer particles and their velocity and acceleration, have a Gaussian distribution about the plume centerline. Thus the model uses two random numbers drawn from a Gaussian distribution: one for the random component of the acceleration due to the ambient turbulence and the other for the random acceleration due to buoyancy.

The model simulations of crosswind-integrated concentrations from a few laboratory and field studies reported in the literature appeared to be satisfactory.

4.3.2 The CSIRO Methods

Instead of accounting for the effects of buoyancy on plume dispersion simply by introducing an extra term into the random walk equation for displacement, Hurley and Physick (1993) compute the vertical velocity of each particle as the sum of the plume velocity due to the buoyancy and initial momentum effect and a stochastic perturbation due to the combined effects of the self generated and ambient turbulence. However, the problem of simulating the entrainment process is not solved since the classical entrainment assumption - the plume radius grows linearly with height - is imposed in both the deterministic and stochastic parts.

The deterministic vertical velocity is obtained by numerically integrating, at each time step, the basic conservation equations (see Section 2) in which the standard assumptions (Boussinesq approximation, top-hat profile and bent over plume) are made. The stochastic wind components are calculated by the Langevin equations for the velocity (Thomson, 1987; see also Chapter 11), namely

$$du_i' = a\,dt + \sqrt{C_0 \varepsilon_a}\, dW \tag{77}$$

where $i = 1,2,3$, u_i' are the Lagrangian velocity fluctuations, a depends on the Eulerian probability density function (PDF) of the turbulent velocity and is determined from the Fokker-Planck equation, C_0 is a numerical constant, dW is a random term, normally distributed (mean 0 and variance dt). For the simulation of plume rise in the CBL, the Gaussian form of the PDF is assumed for the two horizontal components, while a skewed distribution, obtained by a linear

combination of three Gaussian functions, is used for the vertical component. These three functions represent the contribution to the turbulence due to the updrafts, downdrafts and plume self-generation, respectively. In the LSM for passive tracers based on the Langevin equation, the coefficients of the Gaussian functions are obtained by equating the zeroth through third moments of the Eulerian ambient PDF ($0, \sigma_{wa}^2, S_{wa}^3$). In this case, the first three moments of the resulting PDF are equated to $0, \sigma_{wa}^2 + \sigma_{wp}^2, S_{wa}^3$, where σ_{wp}^2 is the velocity variance due to the plume rise effects. The three plume velocity variances are defined, on the basis of the above mentioned classical entrainment assumption, as follows

$$\sigma_{up}^2 = \sigma_{vp}^2 = \left(\beta w_p\right)^2$$
$$\sigma_{wp}^2 = \left(\beta\, w_p / 2\right)^2 \tag{78}$$

where w_p is the particle vertical velocity. The form of the PDF of the vertical velocity fluctuations for simulations in stable conditions is assumed to be Gaussian with the variance and the eddy dissipation rates being calculated as the sum of ambient plus plume rise induced components.

Plume rise computation is terminated either when $\varepsilon_p \le \varepsilon_a$ (convective conditions) or when the buoyancy of a particle becomes less than or equal to zero (stable conditions). The plume penetration of the inversion layer capping the mixing height is simulated letting the plume particles to overcome the mixing height if they do not have yet satisfied the termination condition. When the plume rise calculation is stopped, particles are reflected at the mixing height.

The authors advise of some numerical problems in the first couple of time steps (1 s) after release due, very likely, to the height dependence of $\varepsilon_p \left(= 1.5\, w_p^3 / \Delta h(x)\right)$ on the rise height, which tends to diverge for $\Delta h \propto 0$. The problem was partially solved by imposing, near the stack mouth, $\varepsilon_p \le \sigma_w^2 / (C_0\, \Delta t)$.

Comparisons with CBL water tank dispersion experiments (Willis and Deardorff, 1987), characterized by different values of the dimensionless buoyancy flux F_* - see Equation (42) - were shown. Predicted final plume height Δh and plume entrapment above the CBL were found to be in reasonable agreement with the observed ones, even if a slight overestimation of Δh in three out of four experiments, causing peak entrainment values higher than observed, was found. This could be corrected by changing the value of the entrainment parameter β from 0.6 to 0.7. The overall distribution of concentration compared quite well.

An alternative approach to including plume-rise induced turbulence in a Lagrangian approach, which avoids some of the very-near-source numerical problems above mentioned is contained in the model TAPM (Hurley, 1999, 2000). The equations of conservation of plume volume, buoyancy and momentum flux, G, F_b and F_m, are written in this model - see, for comparison, Equations (2 - 5)

$$\frac{dG}{dt} = 2R\left(\alpha W^2 + \beta U_a W + \gamma u_p E^{1/2}\right)$$

$$\frac{dF_b}{dt} = -s\frac{F_m}{u_p}\left(\frac{1}{2.25}U_a + W\right) \tag{79}$$

$$\frac{dF_m}{dt} = F_b$$

where $G = {T_a}/{T_s}\, u_p R^2$, $F_m = GW$, F_b is defined as in Equation (6), $u_p = \sqrt{U_a^2 + W^2}$ is the plume velocity, E is the turbulent kinetic energy, $a = 0.1$, $\beta = 0.6$ and $\gamma = 0.1$ are the vertical plume, bent-over plume and ambient turbulence entrainment constants, respectively. The initial conditions for F_b and F_m are the same as in Equations (16) and (18),

$$G_s = F_m / v_{s0} \text{ and } R_s = \sqrt{v_{s0} \Big/ \sqrt{u_0^2 + v_{s0}^2}}\ .$$

Equations (79) are based on the model proposed by Glendening et al. (1984), as simplified by Hurley and Manins (1995). Tests on these equations, performed by the authors, showed that they performed as good as the full original ones and collapsed to the Briggs form for a bent-over Boussinesq plume, and to the Briggs vertical plume model equations for calm conditions.

4.3.3 The Weil (1994) Method

This method was designed to deal with CBL dispersion of weakly to moderately buoyant plumes ($F_* \le 0.1$). Also in this method, an extra acceleration term is added in the Langevin equation in order to account for plume rise. This is obtained by numerically solving the conservation Equations (2 - 5) in which the entrainment assumption appearing in Equation (2) is modified to account for the ambient and self-generated turbulence. Consequently, Equation (2) becomes

$$\frac{d}{dt}\left(U_{sc} R^2\right) = 2\beta R U_{sc} \left|w_p\right| + 2\gamma_1 R U_{sc} v_e \tag{80}$$

where the identity $\left(d/dt = U_{sc}\, d/d_{sc}\right)$ was used, v_e is the entrainment velocity and γ_1 an empirical parameter. The first term on the r.h.s of Equation (80) describes the entrainment due to the plume-generated turbulence, whereas the second term accounts for the ambient turbulence. For a jet plume $v_e = v_a$ where

$$v_a = \left(2\varepsilon_a R\right)^{1/3} \tag{81}$$

is the relative velocity of two particles separated by a distance R. Notice that in this approach the radius *R* is defined as "the region enclosing all of the buoyant fluid". For a buoyant plume, having assumed $U_{sc} = U_a$, v_e is given by

$$v_e = \frac{v_a}{1 + \gamma_2\, F_b / \left(U_a v_a^2 R\right)} \tag{82}$$

where γ_2 is another empirical parameter. Defining the dimensionless distance X_* and momentum flux F_{m*} as

$$X_* = \frac{w_* x}{U_a h} \qquad \text{and} \qquad F_{m*} = \frac{F_m}{U_a w_* h^2} \tag{83}$$

Weil (1994) obtained that ambient turbulence becomes effective at a non-dimensional distance $X_a = 1.6\, \alpha_v^{3/5} F_*^{2/5}$ for a buoyant plume and $X_a = 0.6\, \alpha_v^{9/7} F_{m*}^{2/7}$ for a jet, having defined $\alpha_v = v_e / w_p$. Fitting his model to the Willis and Deardorff (1983) observations, this author determined the following values for the unknown parameters: $\gamma_1 = 0.4$, $\gamma_2 = 1$ and $\alpha = 0.49$ or 1.9 for buoyant and jet plumes, respectively. Notice that $\alpha = 0.49$ implies that ambient turbulence starts to dominate when the entrainment velocity is about half the plume velocity ($v_e \approx 0.5 w_p$).

When the plume reaches the temperature inversion height *h* (capping the CBL) and penetration occurs, the vertical plume velocity becomes zero (actually it oscillates about zero) but some plume segments may be brought into the CBL by negative ambient velocities. The buoyant acceleration, due to the fact that the potential temperature is greater than below *h*, provides a positive velocity tending to keep the plume aloft and the ambient velocity (calculated by the Langevin equation) varies randomly and therefore may be either positive or negative.

Weil (1994) also found that, despite the differences in the models, the mean fields computed with this model are very similar to those produced by the Luhar and Britter (1992) model.

4.4 Theoretical Models

4.4.1 The Van Dop (1992) Particle Model for Buoyant Plume Rise

A buoyant plume is defined as the volume, which contains a mixture of ambient and originally released, buoyant fluid. The envelope of the plume is the (imaginary) and in a way, arbitrary boundary of this volume. A fraction of the original buoyant fluid separates from the plume and becomes so remote that it is no longer considered to be part of it. On the other hand the volume of the plume expands due to turbulent intrusions of ambient air resulting in an increasing ambient fraction and consequently, a gradual loss of plume temperature and vertical acceleration.

A Lagrangian 'plume particle' can now be defined as a small entity, which possesses the mean characteristics (velocity, temperature) of the plume. Stochastic fluctuations, directly related to the turbulent intensity within the plume, determine the rate of growth of the plume width and are superimposed on the mean characteristics. Ultimately, due to the entrainment and extrainment processes, the plume (particle) dynamics must converge to the environmental dynamics. Hence, the equation of motion in the vertical dimension for a buoyant plume particle can be formulated as

$$dW = -\frac{W}{T_p}dt + Bdt + \varepsilon_w^{1/2} d\omega_w(t)$$

$$dB = -\frac{B}{T_p}dt - NW^2 + \varepsilon_B^{1/2} d\omega_B(t) \tag{84}$$

$$dX_z = W\,dt$$

(see Van Dop, 1992). Here, W is the plume particle vertical velocity and B is the plume particle buoyancy, defined by

$$B = \frac{g}{T_a}\left(\vartheta_p - \vartheta_a\right) \tag{85}$$

The assumption that the buoyancy of each individual fluid particle is defined by the difference between the particle's temperature and the ambient temperature is a crude one, and in fact the proper buoyancy should be related to the full surrounding temperature field, which includes the temperatures of the other buoyant fluid particles. However, this inclusion would lead to a set of (coupled) Langevin equations for each individual fluid particle, and the attractiveness of the Lagrangian approach would be lost. The Lagrangian time scale of the plume is

assumed to be equal for velocity and buoyancy and is denoted by T_p. The dissipation of velocity and buoyancy is denoted by ε_w and ε_B, respectively. $d\omega_w(t)$ and $d\omega_B(t)$ are random increments in the Lagrangian equations for velocity and buoyancy respectively. The stratification of the environment is given by N - see Equation (15). X_z is the plume particle's vertical position.

The usual assumptions for the random terms are

$$\begin{aligned}
&\overline{d\omega_w(t)} = 0 \\
&\overline{d\omega_B(t)} = 0 \\
&\overline{d\omega_w(t')d\omega_w(t)} = \delta_{tt'}dt \\
&\overline{d\omega_B(t')d\omega_B(t)} = \delta_{tt'}dt \\
&\overline{d\omega_B(t')d\omega_w(t)} = 0
\end{aligned} \tag{86}$$

The last assumption implies that stochastic velocity and buoyancy changes are uncorrelated on the (small) Kolmogorov scales, which may be questionable, but is perhaps not very important for the present consideration. It should be noted that for the mean plume rise, $\overline{X_z}$, the Equations (84) reduce to a deterministic set - due to the properties listed in Equations (86), and thus $\overline{X_z}$ does not depend on the dissipation terms.

In order to simulate a power law behavior for plume rise, which, in the early stage in a calm neutral environment, is confirmed by experimental evidence (see for example Turner, 1973), the Lagrangian time scale must be proportional to t. Assuming $T_p = A_p\,(t + t_o)$, it is retrieved the similarity solution (Csanady, 1973), provided that

$$A_p = 3/4 \tag{87}$$

and

$$t_0 = \left(2r_s / 3\beta B_0\right)^{1/2} \tag{88}$$

The relation with the 2/3 law is imposed by the choice of A_p = 3/4. The initial plume radius and buoyancy are denoted by r_s and B_0, respectively, and β is the plume entrainment constant (~ 0.6). Through the definitions of the plume particle buoyancy, B, and the heat output of the source, Q_h, t_o can be related to the buoyancy flux parameter F_b - see Equation (9) – by

$$\frac{9}{4}B_0^3 t_0^4 = \frac{1}{\beta^2}\frac{F_b}{u} \tag{89}$$

With this choice of parameters the Langevin formulation can be forced to correspond asymptotically ($t \to \infty$) to the classical plume rise formulae.

Plume rise in a turbulent environment was addressed in detail by Netterville (1990) (see Section 2.7.2), who introduced an additional turbulent exchange mechanism, 'extrainment', generated by the ambient turbulence. A logical consequence of his theory for the Lagrangian framework is that if the plume turbulence dominates, the turbulent time scale of the plume, T_p should be applied, whereas if the environmental turbulence dominates, the ambient time scale, T_e , should be used. This view is reflected in an modified expression for the time scale

$$\frac{1}{T_m} = \frac{1}{T_p} + \frac{1}{T_e} \tag{90}$$

The Lagrangian formulation using Equation (90) was compared with Netterville's expression for the mean plume rise and though the Lagrangian formulation results in somewhat lower values, it has the same leveling off behavior in the final stage.

The Lagrangian equations provide also for an independent evaluation of the plume variance or plume width. This requires, however, explicit expressions for the dissipation, ε_w and ε_B in Equations (84). Van Dop (1992) suggests to use the actual particle velocity and buoyancy to parameterize the dissipation and assumes

$$\begin{aligned} \varepsilon_w &= c_1 W^2 / T_p \\ \varepsilon_B &= c_2 B^2 / T_p \end{aligned} \tag{91}$$

where c_1 and c_2 are constants $O(1)$. Numerical solutions for the plume width, σ_z, defined as $\left(\overline{X_z^2} - \overline{X}_z^2\right)^{1/2}$, were obtained, but do not agree with the similarity prediction, $\sigma_z \propto t^{2/3}$.

Alternatively, the dissipation may be parameterized as

$$\begin{aligned} \varepsilon_w &= c_w \left(\frac{t+t_0}{t_0}\right)^{-\alpha_w} \\ \varepsilon_B &= c_B \left(\frac{t+t_0}{t_0}\right)^{-\alpha_B} \end{aligned} \tag{92}$$

Choosing $\alpha_w > 5/3$ and $\alpha_B > 11/3$, and for example equal to 2 and 4, respectively, it can be proven numerically and (in the neutral case, $N = 0$) also analytically that the plume width converges to the similarity prediction

$$\sigma_z = \left(3 c_B t_0^5\right)^{1/2} \left(\frac{t + t_0}{t_0} \right)^{2/3} \tag{93}$$

and the ratio $\sigma_z / \overline{X_z}$ is given by

$$\frac{\sigma_z}{\overline{X_z}} = \left(\frac{3 c_B t_0}{B_0^2} \right)^{1/2} \tag{94}$$

Csanady (1973) suggests (pp. 176-195) that this ratio is approximately 1/3. From this a value for the coefficient c_B of

$$c_B = \frac{B_0^2}{27 t_0} \tag{95}$$

is inferred. Finally, evaluating the plume width in a turbulent environment requires also that the ambient turbulent dissipation rate is considered. As in the case for the Lagrangian time scale - see Equation (90) - Van Dop (1992) suggests the parameterization

$$\varepsilon_m = \frac{\varepsilon_p + \left(T_p / T_e\right)^2 \varepsilon_a}{1 + \left(T_p / T_e\right)^2} \tag{96}$$

where ε_p is given by W^2 / T_p.

The algorithm can without much difficulty be extended to an non-homogeneous and non-stationary ambient turbulence by including height dependent formulations for ambient time scales and dissipation rates and using the appropriate version of the Langevin equations in these conditions. Arbitrary stratification, including a CBL with a capping inversion can be accounted for by introducing a height dependent N.

Though the method contains a number of heuristic elements, the Lagrangian formulation is transparent and computationally straightforward. It is consistent with the classical formulations for plume rise in a calm environment (see Turner, 1973; Briggs, 1969; or Csanady, 1973), but also accommodates more recent Eulerian formulations in a turbulent environment (Netterville, 1990; Nieuwstadt, 1992a,b). This makes it attractive for various practical applications. Yamada (2000) included this algorithm in a modeling system (HOTMAC-RAPTAD) and

examined its performance. He concluded that the overall performance was ‘as least as good as those of the ‘better’ models reported by Hanna et al. (1993)’.

A drawback of the Lagrangian method is that in order to remove the statistical noise, a large number of flow realizations should be evaluated.

4.4.2 Buoyant Plume Rise Described by a Lagrangian Turbulence Model

The research interest in buoyant plume rise is driven by the theoretical aspects of the simulation of the turbulent mixing of fluids with different temperatures. Similarity theory provides parameterizations for the mean plume height and width (Csanady, 1973, Briggs, 1975) if the influence of the ambient turbulence can be neglected, i.e., if the turbulence is generated only by the plume. This applies to the initial stage of plume rise, and for emissions into neutrally stratified ambient flows with a negligible turbulence. However, for practical plume rise calculations, models are required that:

- are computationally not too expensive
- can be applied to both stages of the buoyant plume rise and different ambient conditions
- permit the assessment of fluctuations, i.e., provide also plume statistics

The attempt to derive directly such models leads within the Eulerian framework to Reynolds-averaged Navier-Stokes (RANS) equations, and within the Lagrangian framework to Lagrangian particle models. RANS equation methods (Weil, 1988, Netterville, 1990, Gangoiti et al., 1997) apply parameterizations for terms that are related to the turbulent mixing of the plume and the ambient flow.

By means of Lagrangian methods both the mean plume behavior and the plume statistics can be described in accordance with constraints of the similarity theory and observations. This was demonstrated by van Dop (1992) (see Section 4.4.1) in a first systematic analysis of the description of buoyant plume rise by Lagrangian methods. Alternative methods are described by Anfossi et al. (1993) (see Section 4.2), where also a review can be found on earlier work (see Zannetti and Al-Madani, 1984, Cogan, 1985) to describe buoyant plume rise by means of Lagrangian methods. Lagrangian particle models simulate the plume dynamics, but they require knowledge about the flow field that has to be provided by Eulerian models, or has to be approximated.

Lagrangian turbulence models (LTM) give a full description of both the motion and properties of plume and of the ambient flow. In particular, these Lagrangian equations are constructed consistent with the Eulerian RANS equations. In analogy to direct numerical simulation (DNS) or large eddy simulation (LES) (Nieuwstadt and de Valk, 1987, Nieuwstadt, 1992a,b, Zhang and Ghoniem, 1993, 1994a,b; see Section 3.4), LTM resolves mixing for high-Reynolds number flows avoiding the high computational costs of DNS or LES. We shall derive a buoyant

plume rise model from an LTM, which can be used for regulatory applications and satisfies the constraints (i), (ii) and (iii) considered above.

The Lagrangian description of fluid motion (i.e., of plume- and ambient-air particles) requires Lagrangian equations that are consistent with the Navier-Stokes equations. Two methods are used to date which provide for this consistency: first, the derivation of stochastic Lagrangian equations that are consistent with RANS equations up to second-order (van Dop et al., 1985, Sawford, 1986, Pope, 1994, Heinz, 1997, 1998), and second, the derivation of these equations consistent with an Eulerian velocity PDF (Thomson, 1987). The first approach, which is applied here, requires closure assumptions for the pressure redistribution and dissipation terms in the RANS equations of second-order. Closure assumptions for the pressure redistribution and dissipation terms in the RANS equations are known and relatively well-investigated for buoyant flows (see, e.g., Craft et al., 1996).

Details about the derivation of stochastic Lagrangian equations for buoyant turbulence can be found elsewhere (Heinz, 1997, 1998; Heinz and Van Dop, 1999). Here we present a summary.

The change of particle position dX_i (i = 1, 2, 3), velocity dU_i and potential temperature $d\vartheta_p$ is described by a set of linear stochastic differential equations:

$$\begin{aligned} dX_i &= U_i dt \\ dU_i &= A_i dt + b_{ij} d\omega_j \\ d\vartheta_p &= A^\theta dt + b^\theta d\omega^\theta \end{aligned} \tag{97}$$

where

$$\begin{aligned} A_i &= a_i + G_{ij}\left(U_j - \overline{u_j}\right) + G_i\left(\vartheta_p - \overline{\theta}\right) \\ A^\theta &= a^\theta + G_j^\theta\left(U_j - \overline{u_j}\right) + G^\theta\left(\vartheta_p - \overline{\theta}\right) \end{aligned} \tag{98}$$

The (Eulerian) ensemble average is denoted by overbars and summation over repeated subscripts is assumed. Deterministic changes of the particle velocity are described through the first terms on the right-hand side of Equation (97) with the unknown coefficients $a_i, a^\theta, G_i, G_{ij}, G^\theta$ and G_j^θ. The second terms describe the stochastic force caused by the small-scale turbulence and contains the additional unknown coefficients b_{ij} and b^θ. The properties of $d\omega_j$ and $d\omega^\theta$, random increments for velocity and potential temperature (~ buoyancy) - see Equation (84) - are defined in Section (4.4.1).

Equations (97) can be transformed into a Fokker-Planck equation for the one-point joint velocity-temperature PDF of the flow $P(\boldsymbol{u}, \vartheta, \boldsymbol{x}, t)$ (Gardiner, 1983; Risken, 1984)

$$\frac{\partial P}{\partial t}+\frac{\partial u_i P}{\partial x_i}=-\frac{\partial A_i P}{\partial u_i}-\frac{\partial A^\theta P}{\partial \theta}+\frac{\partial^2 B_{ij} P}{\partial u_i \partial u_j}+\frac{\partial^2 B^\theta P}{\partial \theta^2} \tag{99}$$

with

$$\begin{aligned} B_{ij} &= \frac{1}{2} b_{ik} b_{kj} \equiv \frac{1}{2} C_0 \varepsilon_q \delta_{ij} \\ B^\theta &= \frac{1}{2}\left(b^\theta\right)^2 \equiv \frac{1}{2} C_1 \varepsilon_\theta \end{aligned} \tag{100}$$

The viscous dissipation and potential temperature dissipation are denoted by ε_q and ε_θ, respectively. C_0 and C_1 are constants whose value will be determined later.

From Equation (99) arbitrary moments of velocity and potential temperature can be obtained. In this way we are able to derive a set of equations which are similar to the RANS equations. We can summarize the latter in a suitable approximation up to second order as

$$\frac{d\overline{u_i}}{dt}+\frac{\partial \overline{u_i' u_k'}}{\partial x_k}=-\frac{1}{\rho_a}\frac{\partial \overline{p}}{\partial x_i}+\frac{\mathrm{g}}{T}(\overline{\theta}-\vartheta_a)\delta_{i3}+\nu\frac{\partial^2 \overline{u_i}}{\partial x_k \partial x_k}$$

$$\frac{d\overline{\theta}}{dt}+\frac{\partial \overline{u_k'\theta'}}{\partial x_k}=\kappa\frac{\partial^2 \overline{\theta}}{\partial x_k \partial x_k}$$

$$\begin{aligned} &\frac{d\overline{u_i'\theta'}}{dt}+\frac{\partial \overline{u_i' u_k'\theta'}}{\partial x_k}+\overline{u_k'\theta'}\frac{\partial \overline{u_i}}{\partial x_k}+\overline{u_i' u_k'}\frac{\partial \overline{\theta}}{\partial x_k}=\frac{\mathrm{g}}{T}\overline{\theta'^2}\delta_{i3}+\overline{\frac{p'}{\rho_a}\frac{\partial \theta'}{\partial x_i}} \\ &\frac{d\overline{\theta'^2}}{dt}+\frac{\partial \overline{u_i'\theta'^2}}{\partial x_k}+2\overline{u_k'\theta'}\frac{\partial \overline{\theta}}{\partial x_k}=-2\varepsilon_\theta \\ &\frac{d\overline{u_i' u_j'}}{dt}+\frac{\partial \overline{u_i' u_j' u_k'}}{\partial x_k}+\overline{u_j' u_k'}\frac{\partial \overline{u_i}}{\partial x_k}+\overline{u_i' u_k'}\frac{\partial \overline{u_j}}{\partial x_k}= \\ &=\frac{\mathrm{g}}{T}\left(\overline{u_i'\theta'}\delta_{j3}+\overline{u_j'\theta'}\delta_{i3}\right)+\overline{\frac{p'}{\rho_a}\left(\frac{\partial u_i'}{\partial x_j}+\frac{\partial u_j'}{\partial x_i}\right)}-2\varepsilon_q \end{aligned} \tag{101}$$

Here, T is a boundary-layer reference temperature, and ϑ_a is the mean ambient potential temperature,ν is the molecular viscosity and κ the conductivity. In order to be able to solve Equations (101) we have to make a number of closure assumptions

$$2\nu\overline{\frac{\partial u_p'}{\partial x_k}\frac{\partial u_q'}{\partial x_k}} = \frac{1}{3}\frac{\overline{u_i'^2}}{\tau}\delta_{pq} \tag{102}$$

where τ is a dissipation time scale, which obeys

$$\frac{d\tau}{dt} = C_{\varepsilon 2} - 1 - (C_{\varepsilon 1} - 1)\cdot\frac{2\tau}{q^2}\left\{-\overline{u_k u_l}\frac{\partial \overline{u_l}}{\partial x_k} + \beta g\overline{u_3\theta}\right\} \tag{103}$$

where $C_{\varepsilon 1}$ and $C_{\varepsilon 2}$ are constants equal to 1.56 and 1.9, respectively, and q is twice the turbulent kinetic energy.

$$\varepsilon_\vartheta = \frac{k_4}{2\tau}\overline{\theta'^2} \qquad \varepsilon_q = \frac{q^2}{2\tau} \tag{104}$$

$$\overline{p'\left(\frac{\partial u_i'}{\partial x_j} + \frac{\partial u_j'}{\partial x_i}\right)} = -\frac{k_1}{2\tau}\left(\overline{u_i' u_j'} - \frac{1}{3}q^2\delta_{ij}\right) + k_2 q^2\left(\frac{\partial \overline{u_i}}{\partial x_j} + \frac{\partial \overline{u_j}}{\partial x_i}\right) \tag{105}$$

$$\overline{p'\frac{\partial \theta'}{\partial x_j}} = -\frac{k_3}{2\tau}\overline{u_i'\theta'} \tag{106}$$

In the closure assumptions appear a number of closure constants k_i (i=1-4), which will be determined later.

It can be shown (cf. Heinz, 1997; Heinz and van Dop, 1999) that first and second moment equations derived from Equation (99) can be written similar to Equations (101), provided that the Lagrangian constants appearing in Equations (97) obey the following relationships

$$G_l^\theta = 0 \qquad G^\theta = -\frac{2k_3 - k_1}{4\tau}$$

$$G_i = \frac{g}{T}\delta_{i3} \qquad G_{il} = -\frac{k_1}{4\tau}\delta_{il} \tag{107}$$

$$C_0 = \frac{k_1 - 2}{3} \qquad C_1 = 2k_3 - 2k_4 - k_1$$

An additional consistency requirement is that $k_2 = 0$. Hence we may reformulate the Lagrangian Equations (97) now as

$$dX_z = W\,dt$$

$$dW = -\frac{k_1}{4\tau} W\,dt + B\,dt + \sqrt{\frac{C_0 q^2}{2\tau}}\,d\omega_w$$

$$dB = -\frac{2k_3 - k_1}{4\tau} B dt - N^2 W\,dt + \sqrt{\frac{C_1 (g/T)^2 \overline{\theta^2}}{2\tau}} d\omega^\theta \tag{108}$$

$$\frac{d\tau}{dt} = C_{\varepsilon 2} - 1 - (C_{\varepsilon 1} - 1) \cdot \frac{2\tau}{\overline{u_i'^2}} \left\{ -\overline{u_k u_l} \frac{\partial \overline{u_l}}{\partial x_k} + \beta g \overline{u_3 \theta} \right\}$$

where N is the Brunt- Väisälä frequency and $B = (g/T)(\vartheta_p - \overline{\theta})$. The constants $C_{\varepsilon 1}$ and $C_{\varepsilon 2}$ are related by $C_{\varepsilon 1} = 1 + (C_{\varepsilon 2} - 1)/1.6$ (Heinz,1998). Note that for the evaluation of the Eulerian moments appearing in Equation (108) it is still required to solve Equation (101) numerically.

In order to determine the remaining constants in Equation (97) we have compared the Lagrangian predictions of plume rise with Eulerian approaches (Weil, 1988; Netterville, 1990) in a still environment. This yields

$$C_{\varepsilon 2} = 1 + \frac{3k_1}{8} \cdot \left(\frac{k_3}{k_1} - \frac{1}{2} \right) \tag{109}$$

and

$$k_1 = 4 \left(\frac{3\pi\beta^2}{2} \right)^{1/4} \left(\frac{k_3}{k_1} - \frac{1}{2} \right)^{-1/4} \left[1 - \frac{1}{2} \left(\frac{k_3}{k_1} - \frac{1}{2} \right) \right]^{-3/4} \tag{110}$$

Similarity theory also provides algebraic scaling laws for the variances. Applying these we obtain

$$C_{\varepsilon 2} = 1 + \frac{3}{8} \cdot k_4 \tag{111}$$

Equations (109), (110), and (111) relate four unknown constants, $C_{\varepsilon 2}, k_1, k_3$ and k_4. A value for $C_{\varepsilon 2}$ was found from a comparison of our model results with the LES data of Zhang and Ghoniem (1994a) in stably stratified flow, yielding $C_{\varepsilon 2} = 1.286$. All constants in Equations (108) are now determined.

The full model was evaluated against experimental data collected by Erbrink (1994). The effects of ambient wind shear and stability were considered by solving the parameterized equations for $q^2, \overline{\theta^2}, \overline{u_1 u_3}$ and $\overline{u_3 \theta}$, see Equations (101). Details are given in Heinz and Van Dop (1999).

Figure 7(a) shows a scatter plot of measured plume heights versus the corresponding modeled plume heights in neutral to slightly stable conditions. The figure shows that the agreement between the observed plume heights and our predictions is very good. This means in particular that the model predictions do not only agree with the two-thirds power law, but also estimate correctly the leveling-off of the plume due to ambient stability.

In Figure 7(b) the plume radii are compared. The agreement is still fair, though the scatter has increased. It gives some support for the observation that the 2/3 similarity prediction also holds for the spreading of the plume.

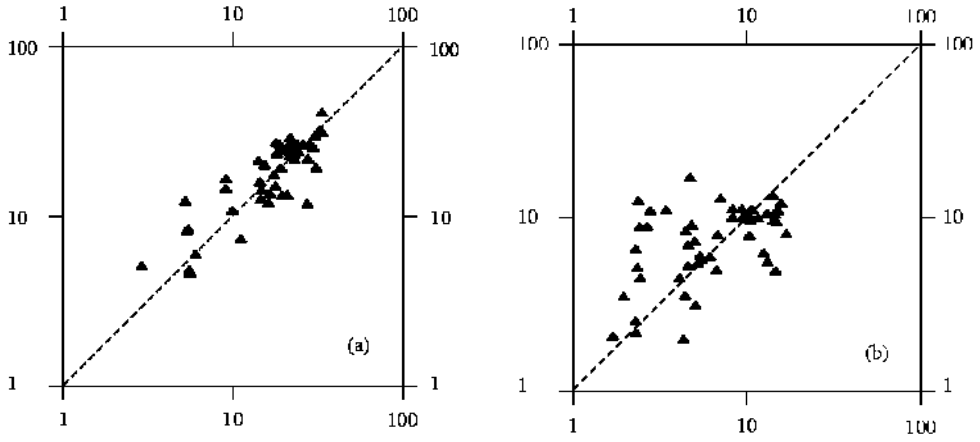

Figure 7. (a) Scatter plot of measured versus modeled normalized mean particle heights, $\overline{X_z} / B_0 \tau_0^2$. B_0 is the initial buoyancy and τ_0 is defined by $\tau_0 = \left(\pi^{1/2} r_s / B_0\right)^{1/2}$. (b) the same comparison but now for the plume widths defined as $\sqrt{\overline{X_z^2} - \overline{X_z}^2} / B_0 \tau_0^2$. Ambient stability conditions during the measurements varied from slightly stable to neutral.

5 Special Cases

All the plume rise estimates discussed in the previous four sections apply to effluents coming out from elevated and isolated sources, without accounting for possible effects of nearby buildings or stacks or of the presence of inversion layers. However, in practice, these situations (and others, like the case of ground level fires, of flares and of the presence of scrubber) need to be investigated since they may affect the plume rise and, consequently, modify the plume trajectory and the ground level concentration distribution. Generally these special topics are treated with "ad hoc" formulations. In this review we will briefly consider the following cases: downwash parameterization, penetration of elevated inversions, plume rise from multiple sources, plume rise from flare stacks, plume rise from fires, plume rise from stacks with scrubber. This review is not exhaustive and will give some examples of possible modeling solutions that are, in general, inserted in regulatory models.

5.1 Downwash Parameterization

In the plume rise computation, a special care must paid to the possible occurrence of downwash effects. These can be classified as:

- stack tip downwash, a possible drag of the effluent in the wake downwind the stack due to the presence of the stack itself
- building downwash, effluent emitted from a stack near a building and brought downward by the flow of air over and around the building

- Stack tip and building downwash cause a decrease in the plume rise because of two concomitant phenomena
- the drag of the effluent in the stack and/or building wake; since this wake extends below the stack outlet, this drag causes the plume to decrease its height
- the increase of the entrainment with ambient air (causing a consequent decrease of buoyancy) due to the wake turbulence

In both cases, the reduced plume rise has the effects of increasing the ground level concentration. In particular, these last may be very high immediately downwind the stack or building if the plume is completely trapped in their wake.

Both stack tip downwash (e.g., Briggs, 1973; Bjorklund and Bowers, 1982; Overcamp, 2001) and building downwash (e.g., Briggs, 1973; Huber and Snyder, 1982; Schulman and Hanna, 1986) are to be considered when the ratio v_s/u is small. In the first case, the buoyancy amount has to be accounted for as well.

The procedures for the correction of the final plume rise, presented in the remainder of this section, do not provide any information about the plume trajectory near the stack outlet. They turn out useful in case one is interested in the prediction of pollutant concentrations in some areas that are at least a few hundreds of meters away from their source.

5.1.1 Stack Tip Downwash

The generally accepted practical rule (Briggs, 1969 and 1973) is that stack downwash will occur if the ratio of effluent speed, v_{s0}, to wind speed, u_0, is less than about 1.5. However Briggs (1969) also suggested that this rule may be relaxed for highly buoyant plume (emitted by modern fossil-fuel power plants and larger industrial stacks). However, stack tip downwash is still an important problem for neutrally buoyant effluents or small industrial emissions. Furthermore, Overcamp (2001) stressed that it is a very important problem in simulating plumes in wind tunnels and towing tanks.

Bjorklund and Bowers (1982) proposed the following expression for the final plume rise corrected for the stack tip downwash, $\Delta h'$

$$\Delta h' = f\ \Delta h \tag{112}$$

where f is a dimensionless parameter calculated with the following procedure:

first, compute the Froude number of the effluent, F_r, defined as

$$F_r = \left(\frac{v_{s0}^2}{2g\sqrt{A_s/\pi}\,(T_{s0} - T_{a0})/T_{a0}} \right)^{1/2} \tag{113}$$

- if $F_r^2 < 3$ then $f = 1$ (no correction);

- if $F_r^2 \geq 3$:
  if $v_s > 1.5\, u_0$ then $f = 1$ (no correction);
  if $u < v_s \leq 1.5\, u_0$ then $f = 3(v_{s0} - u_0)/v_{s0}$;
  if $v_s \leq u_0$ then $f = 0$ (no plume rise).

Snyder and Lawson (1991) modeled the downwash of neutrally buoyant effluent on the immediate lee side of a circular stack in a wind tunnel. They addressed the study to neutrally buoyant plumes solely because, as discussed in the paper, it appears not to be possible to perform the same study for buoyant plumes in a small-scale laboratory. They simulated both sub-critical (Reynolds numbers below the critical Reynolds number, $\cong 2 \times 10^5$) and supercritical (Reynolds numbers above the critical Reynolds number) turbulent flow. Sub-critical Reynolds numbers are typically attained by small-diameter stacks in relatively light winds; supercritical ones are attained by large-diameter stacks in strong winds (supercritical regimes are typical of the majority of full-scale stacks). The downwash characteristics differ markedly in the two regimes. For example, Snyder and Lawson (1991) found that downwash is much more serious in the sub-critical case than in the supercritical one. Furthermore, in the sub-critical regime, downwash begins when the ratio of effluent speed, v_{s0}, to wind speed, u_0, is less than about 1.5; while in the supercritical regimes, downwash begins when such ratio is less than about 1.1. Empirical expressions are provided for vertical plume widths in the sub- and supercritical regimes, for lateral plume widths in the supercritical flow regime (not measured in sub-critical regime), and for plume centroids in the supercritical regime – the centroids in the sub-critical regime are too complex to be fitted by simple expressions.

Overcamp (2001) studied the range of conditions that may lead to downwash in designing simulation of buoyant plumes in wind tunnels and towing tanks. He made a comparison between data on the occurrence of downwash from ten sub-critical model studies and the theory proposed by Tatom (1986) - reference from Overcamp (2001). The Tatom's theory predicts that downwash does not occur if the following implicit relationship is satisfied

$$R' \geq \sqrt{\frac{(3C_D)^{2/3} - 1}{\pi A\left[\frac{1}{F_r^2} + \frac{4B}{\left(4 + B^2\right)^2}\right]}} \tag{114}$$

where:

$$R' = \left(\frac{\rho_{s0}}{\rho_{a0}}\right)^{1/2} \frac{v_{s0}}{u_0}; \quad A = 1 - \exp\left(-\frac{B^2}{2}\right); \quad B = \frac{R'}{\sqrt{\beta + \alpha R'}} \tag{115}$$

and C_D is the drag coefficient. All the ten independent experiments that Overcamp considered were characterized by $R' < 2$. He found that there was good agreement of Tatom's theory with the occurrence of downwash.

5.1.2 Building Downwash

We describe in some detail the method for taking into account the building downwash proposed by Schulman-Scire (Schulman and Scire, 1980; Scire and Schulman, 1980; Schulman and Hanna, 1986), because this method is implemented in both the ISC3 (U.S. EPA, 1995b) and AERMOD (U.S. EPA, 1998) models and is inserted in the CALPUFF code (Scire et al, 1999; http://www.src.com/calpuff/calpuff1.htm) as well. Then, more recently developed building downwash parameterizations will be also presented.

The Schulman-Scire method incorporates the effects of building downwash both on reducing plume rise and on enhancing dispersion parameters.

- $\sigma_{y0} \leq \sigma_{z0}$
  neutral-unstable conditions

the plume rise, $\Delta h_d(x)$, of a downwashed plume is the real solution of the cubic equation

$$\Delta h_d^3 + \left(\frac{3R_0 \Delta h_d}{\beta_1} + \frac{3R_0^2}{\beta_1^2}\right)\Delta h_d = \frac{3F_m x}{\beta_j^2 u_0^2} + \frac{3F_b x^2}{2\beta_1^2 u_0^3} \tag{116}$$

where β_1 is the neutral entrainment parameter (~ 0.6), β_j is the jet entrainment coefficient ($\beta_j = 1/3 + u_0/v_{s0}$), $R_0 = \sqrt{2}\,\sigma_{z0}$ is the dilution radius, and σ_{y0}, σ_{z0} are the horizontal and vertical dispersion coefficients, respectively, at a downwind distance of $3H_b$ (H_b = building height);

- final stable plume rise

$$\Delta h_d^3 + \left(\frac{3R_0 \Delta h_d}{\beta_2} + \frac{3R_0^2}{\beta_2^2} \right) \Delta h_d = \frac{3F_m}{\beta_j^2 u_0 s^{1/2}} + \frac{6F_b}{\beta_2^2 u_0 s} \tag{117}$$

where β_2 is the stable entrainment parameter (~ 0.36). Transitional plume rise during stable conditions is computed with Equation (116) until the final plume height predicted by Equation (117) is obtained.

- $\sigma_{y0} > \sigma_{z0}$

It is necessary to account for the elongated shape of the plume caused by horizontal mixing of the plume in the building wake; the plume can be represented as a finite line source:

- neutral-unstable conditions

the plume rise, $\Delta h_d(x)$, for a line source of length L_e is

$$\Delta h_d^3 + \left[\frac{3L_e}{\pi \beta_1} \right] \Delta h_d^2 + \left(\frac{3R_0 \Delta h_d}{\beta_1} + \frac{6R_0 L_e}{\pi \beta_1^2} + \frac{3R_0^2}{\beta_1^2} \right) \Delta h_d = \\ = \frac{3F_m x}{\beta_j^2 u_0^2} + \frac{3F_b x^2}{2\beta_1^2 u_0^3} \tag{118}$$

- final stable plume rise

$$\Delta h_d^3 + \left[\frac{3L_e}{\pi \beta_2} \right] \Delta h_d^2 + \left(\frac{3R_0 \Delta h_d}{\beta_2} + \frac{6R_0 L_e}{\pi \beta_2^2} + \frac{3R_0^2}{\beta_2^2} \right) \Delta h_d = \\ = \frac{3F_m}{\beta_j^2 u_0 s^{1/2}} + \frac{6F_b}{\beta_2^2 u_0 s} \tag{119}$$

The effective line length is $L_e = \sqrt{2\pi} \left(\sigma_{y0} - \sigma_{z0} \right)$ if $\sigma_{y0} > \sigma_{z0}$; otherwise $L_e = 0$ and Equations (118) and (119) reduce to Equations (116) and (117).

The enhanced dispersion coefficients, σ_{y0} and σ_{z0}, vary with stack height, momentum rise, and building dimensions. As σ_{y0} and σ_{z0} approach zero (e.g., building downwash effects become negligible), Equations (116) to (119) approach the unmodified Briggs (1975) equations. The effect of R_0 and L_e is always to lower the plume height, thereby tending to increase the predicted ground-level concentration.

Hanna et al. (1998) developed a model to describe the lift-off of ground-based buoyant plumes using wind tunnel observations. Special emphasis was given to the development of simple empirical lift-off equations for buoyant plumes, which are trapped in building wakes. The model was developed using wind tunnel observations of plumes for which buoyancy was conserved, but the authors also proposed to use it for plumes whose buoyancy flux varies with distance (phenomenon that can occur due to the presence of aerosols, chemical reactions, and evaporation and condensation processes). Hanna et al. (1998) suggested that the effects of plume lift-off can be accounted for by multiplying the calculated ground-level concentration in the absence of lift-off by an exponential term depending on buoyancy flux. For buoyant plumes trapped in building wakes, the empirical formula that is proposed combines the exponential term with four additional terms related to the spread of plumes in building wakes. Such lift-off formula is incorporated in the HGSYSTEM/UF_6 hazardous gas dispersion code (Hanna and Chang, 1997).

The ADMS code (e.g., see Carruthers et al., 1999) includes a module for building effects based on the model of Hunt and Robins (1982). This module computes the dispersion of pollution from sources near isolated large buildings or closely spaced blocks. The model is able to deal with the influence on turbulent and mean velocity field of an extensive downstream wake. A simplified flow field is defined, based on a well mixed cavity (or recirculating flow region) and a downstream momentum wake. It takes into account the source position and allows for complete or partial entrainment into the recirculating flow region. Within the recirculating flow region concentrations are uniformly calculated. For partially entrained emissions, the entrained and non-entrained components form a two-plume structure downwind. Alternative spread parameters describe dispersion inside and outside the downstream wake.

Flowe and Kumar (2000) showed that a three-dimensional turbulent kinetic energy/dissipation (k-ε) numerical model, FLUENT, can be used as a tool for modeling air flow past a building and stack geometry, and the recirculation cavities associated with wide buildings, and to develop parameterizations useful to air quality modeling needs. These modeling capabilities were proved through the comparison with experimental wind tunnel data generated for several ratios of building width to building heights. Then, the flow field was examined to determine the length of the recirculation cavity as a function of the ratio of building width to building height both in front of and in the rear of the building. The height and length of the front recirculation cavity were parameterized as a function of the ratio of building width to building height. This is a novelty as far as regulatory models are concerned.

Schulman et al. (2000) proposed the Gaussian dispersion model PRIME for plume rise and building downwash. The plume trajectory within the modified fields downwind of the building is estimated using the Zhang and Ghoniem (1993 – see Section 3.4) numerical plume rise model. Such model is based on a numerical solution of the mass, energy and momentum conservation laws. It allows arbitrary

ambient temperature stratification, uni-directional wind shear, and initial plume size. A cavity module calculates the fraction of plume mass captured by and recirculated within the near wake. The captured mass is re-emitted to the far wake as a volume source and added to the uncaptured plume contribution to obtain the far wake concentrations. The PRIME model is implemented within the ISC3 code (Schulman et al., 1997), but it can be implemented in other refined or screening air quality models

5.2 Penetration of Elevated Inversions

Elevated inversions can be divided in thin and thick inversions according to their depth: when the plume cross section is greater than the inversion layer thickness, we have the case of the thin inversion, whereas when the entire plume cross section is contained in the inversion layer, we have the case of a thick inversion.

Plume buoyancy is often large enough to allow plumes to fully or partially penetrate an elevated temperature inversion layer (see Figure 8). Plume material will penetrate an inversion if the temperature excess of a part of the plume at a given height exceeds the temperature change through the layer at the same height. This typically happens during daytime, where the CBL is generally capped by stable air. In the case of a thin inversion, the potential temperature jump $\Delta\vartheta_i$ is the important parameter, whereas in the case of a deep inversion layer the potential temperature gradient, $\partial\vartheta_i/\partial z$ is the characteristic quantity. Consequently, the fate of the plume depends upon these parameters and on the inversion base height (Zannetti, 1990; Weil, 1988). A plume, which is able to completely penetrate the inversion, makes little or no ground level concentration contribution. On the contrary a plume trapped below the inversion can easily be diffused towards the ground bringing about consistent ground-level concentrations (fumigation).

Most of present applied dispersion models (Weil, 1988) only distinguish between complete penetration and no penetration. However many studies (see, for instance: Manins, 1979 or Thompson et al., 2000) have shown that the situation is not so simple and more detailed methods are needed. In particular, Manins (1979) and Zannetti (1990) concluded that a complete plume penetration is almost impossible since, upon reaching the inversion, there will be a part of the plume having insufficient buoyancy for further rise. This was also qualitatively shown by LSM simulations (Zannetti et Al Madani, 1983 and 1984). Thus, it is important to know the fraction of the plume that is trapped.

The simple method provided by Turner (1985) for discriminating between these two cases in presented in Section 5.2.1. Then, we review other penetration models for bent-over plume: first, for a thin inversion, the Briggs (1975), Manins (1979), and Weil (1988) models, see Section 5.2.2; then, for a thick one, the Briggs (1984), and Berkowicz et al. (1986) models, see Section 5.2.3.

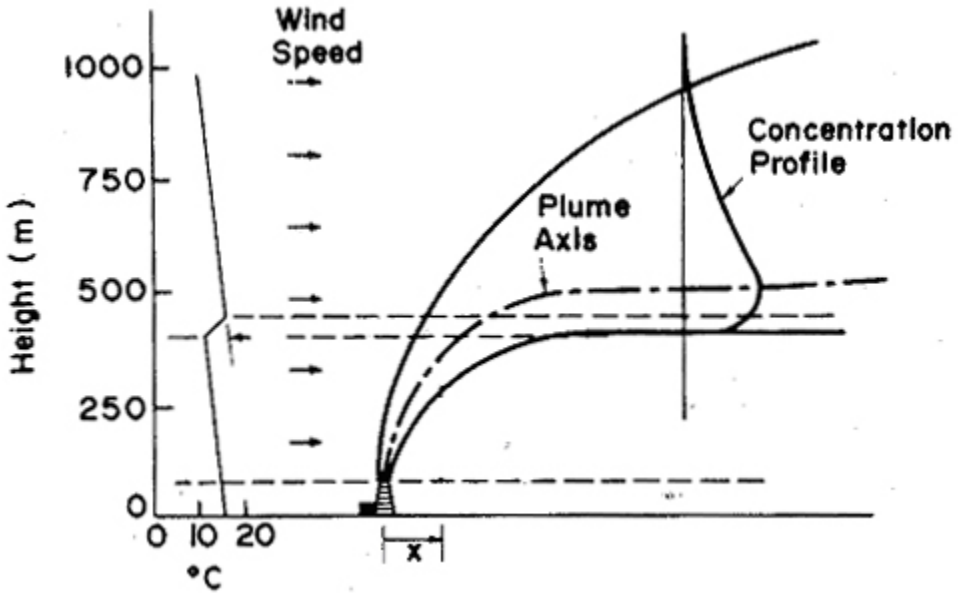

Figure 8. Schematic of the interaction of a buoyant plume and an elevated inversion layer (from Manins, 1979). [Reprinted with permission from Pergamon Press.]

5.2.1 The Turner Procedure

Turner (1985) worked out a pragmatic method using a modification to Briggs (1975, 1984) formulae for computing the final buoyant plume rise by layers and the possible (partial or total) penetration of the plume above the atmospheric thermal discontinuities (such as, typically, the mixing height).

Turner method considers that the plume, during its rise, may meet atmospheric layers of different wind speed and stability. To use this method, one must know or estimate the values of temperature and wind speed close to the stack, on at least two different levels. One at a height between ground level and the stack outlet height, the other at an elevation higher than that reached by the upper edge of the plume at the end of its rise (given by $h_e + 0.5\Delta h$). Obviously, to be able to make optimum use of Turner method, one ought to know the values of temperature and wind speed at numerous intermediate levels, as well as at the previous two levels. Furthermore it is also assumed that the mixing height and the rate of change of potential temperature with height above the mixing height are available.

This procedure for computing the final plume rise consists of the following steps.

1) Calculation of the stack tip downwash factor (*f*) through Bjorklund and Bowers' model (see Section 5.1.1);

- if $f = 0$

Turner method provides a null final plume rise and an effective emission (see item 4 below) equal to the emission at the stack.

- if $f > 0$ we can go onto the following steps;

2) Calculation of the final plume rise keeping into account the plume transit through some atmospheric layers having different characteristics of temperature, wind speed and stability.

We start computing the final plume rise, by using a modification to Briggs (1975, 1984) formulae and the meteorological parameters of the atmospheric layer that includes the stack outlet. If either the obtained final plume rise (in neutral or unstable conditions) or the upper edge of the plume (in stable conditions) does not overtake the top of the layer containing the stack outlet, the calculated final plume rise is the results of the first part of Turner method. If neither of them does, we have to compute the residual buoyancy, and use it to repeat the computation procedure of the final plume rise of the next layer; the new plume rise has the same fate as the previous one. The process goes on from layer to layer till the result will be obtained.

3) The final plume rise computed through the procedure illustrated at point 2) is adjusted by the stack tip downwash factor (see Section 5.1.1).

4) To calculate the penetration of the plume above atmospheric thermal discontinuities, this procedure assumes that a fraction f' ($0 \le f' \le 1$) of the total emission, Q, remains trapped below the base of the thermal discontinuity, placed at the height h_t, and affects the concentration measured by receptors below this height. The product $f'Q$ is known as the "effective emission".

As far as f' is concerned two options are possible:

a) $f' = 1$; this means that this option disregards the penetration of the plume above the thermal discontinuity, but takes only into account the modification made to the plume rise;

b) $f' \neq 1$ and the modified plume rise are calculated with the method discussed below.

Option b) can be chosen only if h_t is greater than the distance of receptors from ground level. With this method, three possibilities are considered, depending on the values taken by the parameters

$$t_p = h_e + 0.5\Delta h \tag{120}$$

and

$$b_p = h_e - 0.5\Delta h \tag{121}$$

assumed by Turner to represent the upper and the lower edge of the plume. These three possibilities are:

- if $t_p \le h_t$, no penetration of the plume above the thermal discontinuity is assumed, i. e. $f' = 1$;
- if $b_p \ge h_t$, the entire plume is assumed to penetrate above the thermal discontinuity, i. e. $f' = 0$; no concentration is measured by receptors;
- in the intermediate case, i. e. $b_p < h_t < t_p$, Turner proposes

$$0 < f' = \frac{h_t - b_p}{\Delta h} < 1 \tag{122}$$

and

$$\Delta h'' = \frac{1 + f'}{2}\Delta h \tag{123}$$

as the actual plume rise, instead of Δh.

This plume rise/partial penetration technique provides a computationally simple solution for engineering calculations. However, the problem of correctly modeling partial penetration is still wide open.

One can observe that, since this method requires a detailed knowledge of the various atmospheric layers crossed by the plume (e.g., coming from vertical profile observations), it would be similarly simpler to solve directly the conservation equations as mentioned in Section 3. However, this method was recalled here since it is incorporated in some dispersion models, like, for instance, in the TUPOS model (Turner et al., 1986), in the PTSRCE preprocessor program of UAM-V (U.S. EPA[12]), and in the SAFE_AIR package (Canepa et al., 2000[3]) as a user option.

5.2.2 Thin Inversion

For a vertical plume, Briggs (1975) predicts that a thin inversion layer can be completely penetrated if the mean temperature excess of the plume at height h' ($h' = h_t - z_s$) exceeds the temperature jump $\Delta\vartheta_i$. Defining $b_i = (g/\vartheta)\Delta\vartheta_i$, complete penetration occurs if

[1] http://www.epa.gov/scram001,
[2] http://uamv.saintl.com/
[3] http://155.207.20.121/mds/bin/show_long?SAFE_AIR

$$F_b > 0.019 b_i^{3/2} \left(h'\right)^{5/2} \tag{124}$$

for a buoyant plume, and

$$F_m > 0.25 b_i \left(h'\right)^3 \tag{125}$$

for a jet. This last equation is based upon experimental results by Vadot (1965).

For bent over buoyant plumes the finite depth of the plume cannot be neglected and, consequently, partial penetration is more likely than complete penetration. The Briggs (1975) model considers the plume buoyancy depletion during the inversion traverse. Defining an equilibrium height with respect to the top of the stack, z'_{eq}, where its buoyancy flux is equal to zero and assuming the plume cross-section to be rectangular with a depth equal to the rise Δh, and a width equal to 0.5 Δh, z'_{eq} is found to be (Briggs, 1975; Weil, 1988):

$$\frac{z'_{eq}}{h'} = \frac{2}{3}\left(1 + 9\pi P_b\right)^{1/2} \tag{126}$$

where the dimensionless buoyancy flux P_b is given by

$$P_b = \frac{F_b}{U_a b_i h'^2} \tag{127}$$

The percentage of plume trapped by the inversion and thus diffused downwards is

$$f' = 1 - P_b = \frac{h'}{z'_{eq}} - 0.5 \tag{128}$$

From which the following simple criteria derive:

- $z'_{eq} < \frac{2}{3} h'$, no penetration ($f' = 1$);
- $\frac{2}{3} h' < z'_{eq} < 2h'$, partial penetration - f' is given by Equation (128);
- $z'_{eq} > 2h'$, complete penetration ($f' = 0$).

For bent over jets, substantial inversion penetration may be assumed (Briggs, 1975) when

$$F_m > 2.2 \beta^2 u_0 b_i^{1/2} \left(h'\right)^{5/2} \tag{129}$$

The Manins (1979) model is based on the assumption that the density or temperature is normally distributed in a bent over buoyant plume when its centerline reaches the inversion. As in the previous Briggs (1975) model, the inversion is idealized as a jump of zero thickness. Defining $\Delta\vartheta_m$ to be the maximum excess temperature, Manins also assumed that penetration starts when $\Delta\vartheta_m = \Delta\vartheta_i$, and found that this happens if

$$P_b = 0.08 \tag{130}$$

He suggested that partial penetration would occur, for the part of the plume with $\Delta\vartheta > \Delta\vartheta_i$, when $P_b > 0.08$. Accounting for the effects of the momentum overshoot of the plume and the re-entrainment back into the plume of material trapped within the inversion, the above condition leads to the following expression for the fraction of the plume trapped in the inversion layer

$$f' = \frac{0.08}{P_b} - \left(P_b - 0.08\right) \tag{131}$$

Weil (1988) compared laboratory observations (see Figure 9) of inversion penetration by Manins (1979) and Richards (1963) and noted that Manins model, Equation (131), fits reasonably well his data but overestimates most of Richards data while Briggs model, Equations (126) and (128), overestimates part of the observed f'. Weil argues that these differences between models and observations can possibly be due to some different configurations in the experimental conditions between the two experiments and, in particular, of the ratio $\Delta h_i / h'$, where Δh_i is the finite thickness of the inversion layer. As a consequence, Weil (1988) considers the effect of Δh_i on the plume penetration capacity and of a different temperature distribution. He found that the fraction of the plume below the inversion top, $h' + \Delta h_i$, is

$$f' = 1 - \frac{1}{\pi}\left[\cos^{-1}\lambda - \lambda\left(1-\lambda^2\right)^{1/2}\right] \tag{132}$$

where

$$\lambda = \frac{1+\delta-\eta_{eq}}{\beta'\eta_{eq}} \tag{133}$$

with $\eta_{eq} = \dfrac{z'_{eq}}{h'}$, and $\delta = \dfrac{\Delta h_i}{h'}$.

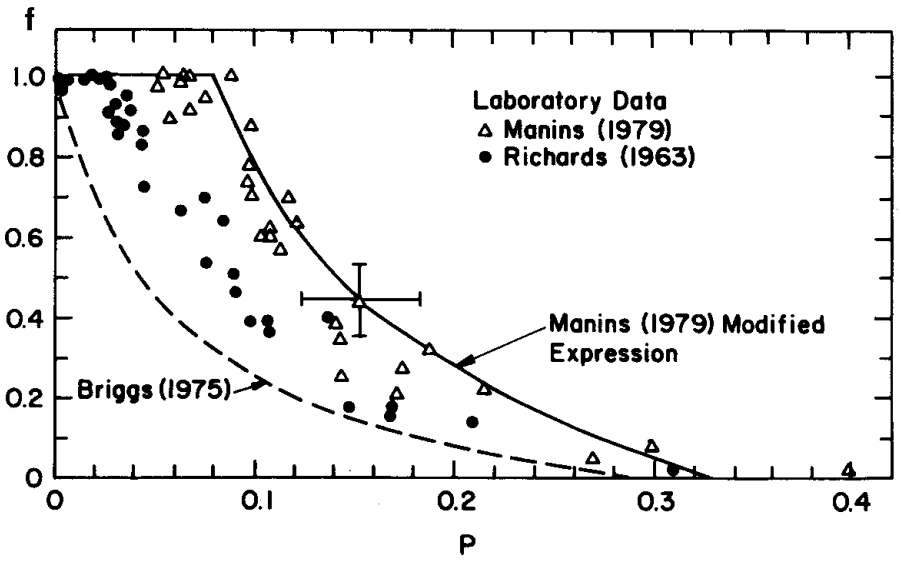

Figure 9. Models and laboratory measurements of the fraction of a plume trapped by an elevated inversion as a function of the dimensionless buoyancy flux P (adapted from Weil, 1988). [Reprinted with permission from American Meteorological Society]

5.2.3 Thick Inversion

In this case the reference inversion height h', to calculate penetration and trapping probabilities of occurrence, is the height of the inversion base. Briggs (1975, 1984) considered the simple case in which s is constant with height. He also assumed that plume equilibrium height is given by Equation (44), namely

$$z'_{eq} = 2.6\left(\frac{F_b}{su_0}\right)^{1/3} \tag{134}$$

in which s is computed from $d\vartheta_i/dz$. To estimate the fraction of the plume trapped $f' = 1 - P_b$, he used Equation (128), obtaining

- $z'_{eq} < \frac{2}{3}h'$, no penetration ($f' = 1$);
- $\frac{2}{3}h' < z'_{eq} < 2h'$, partial penetration - f' is given by Equation (128);
- $z'_{eq} > 2h'$, complete penetration ($f' = 0$).

Briggs' (1984) model gives conservative estimates since the plume initially rises in an atmosphere with $s = 0$, in which it should not experience any buoyancy depletion.

Berkowicz et al. (1986) considered this aspect. By assuming that the process of buoyancy reduction initiates only when the upper boundary of the plume arrives at h', they proposed the following equation for the ratio z'_{eq}/h'

$$\frac{z'_{eq}}{h'} = \left[2.6^3 P_s + (2/3)^3\right]^{1/3} \tag{135}$$

where

$$P_s = \frac{F_b}{U_a N_i^2 h'^3} \tag{136}$$

5.3 Plume Rise from Multiple Sources

When several stacks are located close to each other, the resulting plume rise is different from that of a single stack. Plumes coming from the various stacks generally merge during the rise stage thus causing enhanced rise due to reduced ambient air entrainment and increased buoyancy. Consequently, ground level concentration is reduced. This enhanced plume rise was observed both in laboratory experiments and in the field (Manins et al., 1992). In general the enhancement is greater in the case of flow parallel to the stacks than in the normal flow and, in both cases, the plume rise exceeds that of a single plume (Anfossi, 1985). Overcamp and Ku (1988) also confirmed that enhancement is a function of the angle between the direction of the wind and the line of stacks, finding that the rise is larger when the angle is small. In the same way, also plumes coming from cooling towers (Bornoff and Mokhtarzadeh-Dehghan, 2001) or from multiple fires (Trelles et al., 1999b) may merge and experience enhanced rise.

Briggs (1975) provided a semi empirical formulation for determining the plume rise in the case of stacks of equal height and buoyancy flux. He defined the enhancement factor, E_n, as the ratio of the plume rise from n stacks to that of one stack, whose expression is the following

$$E_n = \left(\frac{n+S}{1+S}\right)^{1/3}, \qquad S = \left(\frac{n-1}{n^{1/3}\Delta h_1 / d}\right)^{3/2} \tag{137}$$

where d is the spacing between the stacks and Δh_1 is the plume rise from a single stack.

Anfossi et al. (1978) developed and tested (Anfossi et al. 1979; Anfossi, 1982, 1985; Sandroni et al., 1981) a virtual stack concept that allows two or more stacks of different buoyancy and heights to be merged. Their model for the plume rise from multiple sources is expressed by the following equation

$$\Delta H^N = H_i + C\sum_{j=1}^{N}\left\{F_j^{1/3} - \left[\left(H_i - H_j\right)/C\right]^3\right\}^{1/3} \tag{138}$$

in which

$$H_i = H_{\max} + \frac{\Delta H_{\min} - \left(H_{\max} - H_{\min}\right)}{1 + \left[\Delta H_{\min} - \left(H_{\max} - H_{\min}\right)\right]/D} \tag{139}$$

is the merging point height, $\Delta H_{\min}$ is the maximum single plume rise from lowest stack $H_{\min}$, $C = \Delta H_{\min} / F_{\min}^{1/3}$ and $D = (n-1)d$. In the case of stacks of equal height and buoyancy flux, Equations (138) and (139) reduce to

$$E_n = \frac{1 + n^{1/3}\left(\Delta h_1 / D\right)}{1 + \left(\Delta h_1 / D\right)} \tag{140}$$

Anfossi (1985) and Manins et al. (1992) demonstrated that Equations (137) and (140) give almost equal results.

5.4 Plume Rise from Flare Stacks

A flare stack is a vent gas stack with a small pilot flame at the stack exit. Combustible vent gases flowing from the stack exit are ignited by the pilot flame and burned in the open atmosphere just above the stack exit. The hot, combusted gas plume then rises and disperses in the atmosphere just as does any hot, buoyant plume. Flare stacks are widely used in industrial plants; in particular, flare stacks are an essential safety requirement in hydrocarbon processing facilities.

By means of direct observation, Leahey and Davies (1984) showed that the entrainment of ambient air into the flare plume is similar to what found in stack plumes and that the flare plumes rise according to the "two-third" law.

The SCREEN3 model (U.S. EPA, 1995a) deals with flare. Buoyancy flux for flare release is estimated from

$$F_b = 1.66\ 10^{-5}\ Q_f \tag{141}$$

where Q_f is the total heat release rate of the flare (cal s^{-1}). This formula - see Equation (9) - was proposed by Briggs (1969). The value of the constant was derived fixing T_a = 293 K, ρ_a = 1205 g m^{-3}, c_p = 0.24 cal g^{-1} K^{-1}, and assuming the following relationship between Q_f and the sensible heat release rate Q_h: $Q_h = 0.45\ Q_f$. The sensible heat rate is based on the assumption that 55 % of the total heat released is lost due to radiation (Leahey and Davies, 1984). The buoyancy flux

for flares is calculated in SCREEN by assuming effective stack parameters of v_{s0} = 20 m s^{-1}, T_{s0} = 1273K, and solving for an effective stack diameter, $d_s = 9.88\ 10^{-4}\ (Q_h)^{0.5}$.

5.5 Plume Rise from Fires

Environmental consequences of large fires are of interest since the rise and transport of combustion products can distribute potentially hazardous materials over a wide area (McGrattan et al., 1996). Plume rise simulation from fires is not straightforward. For example, the life cycles of a forest fire includes an initial developing stage with large increases in heat generation and pollutant emissions rates, followed by a stage of decreasing values. Therefore, the source parameters of a forest fire are usually not constant. The magnitude of the variation in heat generation and emission rates may be two orders of magnitude over the course of burn (Scire et al, 1999).

Various models dealing with plume rise from fires are available in the literature. For instance Manins (1985) considered plumes from fires from thermonuclear explosions (direct bomb fires, incineration of the immediate blast area and injection from fires which spread from the blast area). The prediction of fire plume-rise was based on the Boussinesq buoyant plume model of Morton et al. (1956) since this was shown by Turner (1973) and Briggs (1975) to give good results for small to large heat sources when the ambient wind is light (see also Section 2.1).

Recently McGrattan et al. (1996) presented a LES model of smoke plumes generated by large outdoor pool fires transported by a uniform ambient wind. This model was extended by Trelles et al. (1999a) to deal with the problem of large-scale fire plumes in the presence of winds, which vary, in the vertical direction. A further extension performed by Trelles et al. (1999b) investigated multiple fire plumes. In fact large scale fire scenarios commonly involve multiple combustion sources: the class of problems considered excludes fires large enough to alter the prevailing atmosphere, but it allows for fires sufficiently strong to interact with each other and to have local atmospheric influence.

Also some regulatory computer codes include the treatment of plume rise from fires. For example, the FIREPLUME code (Brown et al., 1999) and the CALPUFF code (Scire et al, 1999; http://www.src.com/calpuff/calpuff1.htm) that are briefly described below.

FIREPLUME (Brown et al., 1999) is able to simulate atmospheric dispersion and air quality impacts from fires. FIREPLUME deals with plume rise by means of the MCLDM Lagrangian particle model (Brown et al, 1996). The framework for treating source buoyancy closely follows from the “two-thirds” law, which is applicable in cases where the buoyant source has low initial momentum. Fires clearly fall into this category (Weil, 1982). Although the “two-thirds” law is

primarily used for stack emissions, its extension to fire buoyancy is straightforward. The plume rise relationships are incorporated into MCLDM to provide a mean vertical velocity for the individual particles. The vertical dispersion from a variety of buoyant release scenarios can be evaluated, from intensely buoyant sources typical in actively burning forest fires to very low buoyancy sources, such as, in the residual stages of smoldering biomass.

In CALPUFF (Scire et al, 1999; http://www.src.com/calpuff/calpuff1.htm) the area source plume rise model is formulated to calculate the rise of buoyant plumes resulting from forest fires, the burning of leaking oil, and other type of buoyant area sources. The model is designed to be applicable to the following conditions: 1) all types of ambient temperature stratifications; 2) all types of wind stratifications (wind shear is important because the forest fire plume starts at ground where there is a zone of large velocity gradients in the vertical); 3) any size of finite emission source; 4) include the effects of plume radiative heat loss; and 5) Boussinesq approximation is not assumed.

5.6 Plume Rise from Stacks with Scrubber

Desulfurization techniques have often been adopted for either the combustibles (e.g., coal cleaning) or the flue gas (scrubbers). The latter technique seems by far the most cost effective for SO_2 emission reduction. Most flue gas desulfurization devices employ a wet scrubbing technique in which a $Ca(OH)_2$ solution is used for partial removal of SO_2.

Plumes from stacks with scrubbers are frequently modeled using the same techniques as the other plumes. Schatzmann and Policastro (1984) reviewed the problem of evaluating Δh for stacks with scrubbers, concluding that “the significant moisture content of the scrubbed plume upon exit leads to important thermodynamic effects during plume rise that are unaccounted for in the usual dry plume rise theories”.

Plume rise models for wet plumes (e.g., cooling tower plumes) have been developed by Hanna (1972), Weil (1974), and Wigley and Slawson (1975). Even these formulations, however, are inappropriate for scrubbed plumes, according to Schatzmann and Policastro (1984), because of the simplifications they adopt. Sutherland and Spangler (1980) compared observed plume rise heights for scrubbed and unscrubbed plumes and evaluated the performance of several plume rise formulations. They found that simple plume rise formulae are questionable even for dry plumes, while moisture effects in scrubbed plumes increase the plume buoyancy and almost compensate for the loss of plume rise due to the temperature decrease induced by the scrubbing system. Plume rise of moist plumes was reviewed by Briggs (1984).

Schatzmann and Policastro (1984) recommend integral-type models for scrubbed plumes, with the additional requirement of avoiding some common

simplifications such as the linearization of the equation of state, first-order approximations in the calculation of the local saturation deficit, and the Boussinesq approximation.

References

Abraham, G. (1970): Round buoyant jet in cross-flow. Paper presented at the *5th International Conf. Water Pollut. Res.*, San Francisco, CA.

Anfossi, D., G. Bonino, F. Bossa, and R. Richiardone (1978): Plume rise from multiple sources: a new model. *Atmos. Environ*., **12**:1821-1826.

Anfossi, D., G. Bonino, and R. Richiardone (1979): An application of plume rise model for multiple sources to the cooling tower plumes of John E. Amos Power Plant. *Il Nuovo Cimento*, **2C,N.4**:488-498.

Anfossi, D. (1982): Plume rise measurements at Turbigo. *Atmos. Environ*., **16**:2565-2574.

Anfossi, D. (1985): Analysis of plume rise data from five TVA Steam Plants. *J. Clim. App. Met*., **24**:1225-1236.

Anfossi, D., E. Ferrero, G. Brusasca, A. Marzorati, and G. Tinarelli (1993): A simple Way of Computing Buoyant Plume Rise in Lagrangian Stochastic Dispersion Models, *Atmos. Environ.*, **27A**:1443-1451.

Anfossi, D. (2000): Jet plume rise description in Lagrangian Stochastic Models. ICGF Rapp. Int. No 414/2000, 9 pp.

Arya, P. S., (1999) *Air pollution meteorology and dispersion*. Oxford University Press, New York. http://www.oup-usa.org/

Berkowicz, R., H.R. Olesen, and U. Torp (1986): The Danish Gaussian air pollution model (OML): description, test and sensitivity analysis in view of regulatory applications. *Air Pollution Modeling and Its Application V*. C. De Wispelaere, F.A. Schiermeier, and N.V. Gillani Editors., Plenum, New York, 453-481.

Bjorklund, J.R., and J.F. Bowers (1982): User's instruction for the SHORTZ and LONGZ computer programs, Volumes I and II. EPA Document EPA-903/9-82-004A and B, U.S. EPA, Middle Atlantic Region III, Philadelphia, Pennsylvania, USA.

Bornoff R.B. and Mokhtarzadeh-Dehghan M.R. (2001) A numerical study of interacting buoyant cooling-tower plumes. *Atmos. Environ.*, **35**, 589-598

Briggs, G.A. (1969): Plume rise. AEC Crit. Rev. Ser., TID-25075. Springfield (VA), pp. 80.

Briggs, G.A. (1972): Chimney plumes in neutral and stable surroundings. *Atmos. Environ.* **6**:507-510.

Briggs, G.A. (1973): Diffusion estimation for small emission. In Atmospheric Turbulence and Diffusion Laboratory 1973 Annual Report. (NOAA/ATDL, Oak Ridge, TN, publication no. ATDL-106, pp 739-747

Briggs, G.A. (1975): Plume rise predictions. In: Lectures on air pollution and environmental impact analyses, D. Haugen (editor). Workshop proceedings, Boston, Massachusetts, September 29 – October 3, pp. 59-111, American Meteorological Society, Boston, Massachusetts, USA.

Briggs, G.A. (1984): Plume rise and buoyancy effects. Technical Report Atmospheric Science and Power Production, DOE/TIC-27601, edited by D. Randerson, U.S. Department of Energy, Washington, D.C.

Bringfelt, B. (1969): A study of buoyant chimney plumes in neutral and stable atmospheres. *Atmos. Environ*., **3**:609-623.

Brown, D.F., W. E. Dunn, A.J. Policastro, and D. Malony (1996): FIREPLUME model for plume dispersion from fires: applications to UF6 cylinder fires, ANL/EAD-PM69.

Brown, D.F., W.E. Dunn, M.A. Lazaro, and A.J. Policastro (1999): The FIREPLUME model: tool for eventual application to prescribed burns and wildland fires. *The joint fire science conference and workshop*. Boise,. Idaho, June 15-17, 1999.

Brummage, K.G. (1966): The calculation of atmospheric dispersion from a stack. Stichting CONCAWE, The Hague, The Netherlands.

Canepa, E., F. Modesti, and C.F. Ratto (2000): Evaluation of the SAFE_AIR code against air pollution field and laboratory experiments. *Atmos. Environ*., **34(28):**4805-4818.

Carpenter, S.B., T.L. Montgimery, J.M. Leavitt, W.C. Colbaugh, and F.W. Thomas (1971): Principal plume dispersion models: TVA power plants. *J. Air Pollut. Control Ass.*, **21**:491-495.

Carras, J.N., and D.J. Williams (1984): Experimental studies of plume dispersion in convective conditions – 1. *Atmos. Environ*., **18**:135-144.

Carruthers, D.J., A.M. Mckeown, D.J. Hall, and S. Porter (1999): Validation of ADMS against Wind Tunnel Data of Dispersion from Chemical Warehouse Fires. *Atmos. Environ*., **33**:1937–1953.

Chiang H.C. and Sill B.L. (1985): Entrainment models and their application to jets in a turbulent cross flow. *Atmos. Environ*., **19**:1425-1438

Cogan, J.L. (1985): Monte Carlo simulation of a buoyant dispersion. *Atmos. Environ*., **19**:867-878.

Craft, T.J., N.Z. Ince, and B.E. Launder (1996): Recent Developments in Second-Moment Closure for Buoyancy-Affected Flows. *Dynamics of Atmos. and Oceans*, **23**:99-114.

Csanady, G.T. (1973): Turbulent Diffusion in the Environment. *Geophysics and Astrophysics Monographs, Vol. 3.* R. Reidel Publishing Company, Dordrecht-Holland, Boston-USA.

Djurfors, S.G. (1977): On the rise of buoyant plumes in turbulent environments. Syncrude Canada Ltd. Professional Paper 1977-4.

Djurfors, S.G. (1983): Discussion of effective source flux parameters for use in analytical plume rise models. *Atmos. Environ*., **17**:197-198.

Erbrink, H.J. (1994): Plume Rise in Different Atmospheres: A Practical Scheme and some Comparisons with LIDAR Measurements. *Atmos. Environ*., **28**:3625-3636.

Fay, J.A., M.P. Escudier, and D.P. Hoult (1970): A correlation of field observations of plume rise. *J. Air Pollut. Control Assoc.*, **20**:391-397.

Finardi, S., G. Tinarelli, A. Nanni, D. Anfossi, E. Ferrero, S. Trini Castelli (2001): In situ diagnostic or nested prognostic meteorological models to drive dispersion simulations in complex area: a comparison in a real application. Air Pollution Modelling and its Applications XIV, S.E. Gryning and F.A. Schiermeier eds., Kluwer Academic / Plenum Press, New York.,641-649

Flowe, A.C., and A. Kumar (2000): Analysis of velocity fields and dispersive cavity parameters as a function of building with to building height ratio using a 3-D computer model for squat buildings. *Journal of Wind Engineering and Industrial Aerodynamics*, **86**:87-122.

Gangoiti, G., J. Sancho, G. Ibarra, L. Alonso, J.A. García, M. Navazo, N. Durana, and J.L. Ilardia (1997): Rise of Moist Plumes from Tall Stacks in Turbulent and Stratified Atmospheres. *Atmos. Environ*., **31A**:253-269.

Gardiner, C.W. (1983): *Handbook of Statistical Methods.* Springer Verlag, Berlin, Heidelberg, New York, Tokyo.

Glendening, J.W., J.A. Businger, and R.J. Farber (1984): Improving plume rise prediction accuracy for stable atmospheres with complex vertical structure. *J. Air Pollut. Control Ass.*, **34**:1128-1133.

Golay, M.W. (1982): Numerical modeling of buoyant plumes in a turbulent stratified atmosphere. *Atmos. Environ*., **16**:2373-2381.

Graziani G., Martilli A., Pareschi M.T. and Valenza M. (1997) Atmospheric dispersion of natural gases at Vulcano island. Journal of Volcanology and Geothermal Research, 75, 283-308

Hanna, S.R. (1972): Rise and condensation of large cooling tower plumes. *J. Appl. Meteor.*, **11**:793-799.

Hanna, S.R., G.A. Briggs, and R.P. Jr. Hosker, (1982): Handbook on atmospheric diffusion. Prepared for the Office of Health and Environmental Research, Office of Energy Research, U.S. Department of Energy, DOE/TIC 11223, J.S. Smith, Publication Editor.

Hanna, S.R., Chang J.C. Strimaitis D.G. (1993): Hazardous gas model evaluation with field observations. *Atmos. Environ*., **27A**:2265-2285.

Hanna, S.R. (1994): Lecture on Air quality modeling over short distances. College on atmospheric boundary layer and air pollution modelling. ICTP Trieste, 16 May-3 June 1994.

Hanna, S.R., and J.C. Chang (1997): HGSYSTEM/UF_6 model enhancements for plume rise and dispersion around buildings, lift-off of buoyant plumes, and robustness of numerical solver. K/SUB/93-XJ947/R, OSTI, P.O. Box 62, Oak Ridge, TN 37831.

Hanna, S.R., G.A. Briggs, and J.C. Chang (1998): Lift-off of ground-based buoyant plumes. *Journal of Hazardous Materials*, **59**:123-130.

Heinz, S. (1997): Nonlinear Lagrangian Equations for Turbulent Motion and Buoyancy in Inhomogeneous Flows. *Phys. Fluids*, **9**:703-716.

Heinz, S. (1998): Time Scales of Stratified Turbulent Flows and Relations between Second-Order Closure Parameters and Flow Numbers. *Phys. Fluids*, **10**:958-973.

Heinz, S., and H. van Dop (1999): Buoyant plume rise described by a Lagrangian turbulence model. *Atmos. Environ.*, **33**:2031-2043.

Henderson-Sellers, B., and S.E. Allen (1985): Verification of the plume rise/dispersion model USPR: plume rise for single stack emissions. *Ecological Modelling*, **30**:209-277.

Hewett, T.A., J.A. Fay, and D.P. Hoult (1971) Laboratory experiments of smokestack plumes in a stable atmosphere. *Atmos., Environ.,* **5**:767-789.

Holland, J.Z. (1953): Meteorology survey of the Oak Ridge area. ORO-99. U.S. At. Energy Comm., Oak Ridge, Tennessee.

Hoult, D.P., and J.C. Weil (1972): A turbulent plume in a laminar crossflow. *Atmos. Environ*., **6**:513-531.

Huber, A.H., and W.H. Snyder (1982): Wind tunnel investigation of the effects of a rectangular-shaped building on the dispersion of effluents from short adjacent stacks. *Atmos. Environ*., **17**:2837-2848.

Hunt, J.C.R., and A.G. Robins (1982): A model for assessing dispersion of plumes from sources in the vicinity of cuboid shaped buildings. Proceedings of the EUROMECH Conference on Surface Mounted Bluff Bodies in Turbulent Boundary Layers, Lisbon.

Hurley, P.J., and W. Physick (1993): Lagrangian particle modelling of buoyant point sources: plume rise and entrapment under convective conditions, *Atmos. Environ.*, **27A**: 1579-1584.

Hurley, P.J., and P.C. Manins (1995): Plume rise and enhanced dispersion in LADM. ECRU Technical Note No.4, CSIRO Division of Atmospheric Research, Australia.

Hurley, P.J. (1999): The Air Pollution Model (TAPM) Version 1: Technical Description and Examples. CSIRO Atmospheric Research Technical Paper No. 43.

Hurley, P.J. (2000): TAPM Technical Report. TAPM web page http://www.dar.csiro.au/res/aq/Tapm/default.htm.

Hurley, P.J., A. Blockley, and K. Rayner (2001): Verification of a prognostic meteorological and air pollution model for year-long predictions in the Kwinana industrial region of Western Australia. *Atmos. Environ.*, **35**:1871–1880.

Janicke, L. (1983): Particle simulation of inhomogeneous turbulent diffusion. In: Weber, B. (Ed.), Air Pollution Modeling and its Application II. Plenum Press, New York, 527-535. http://www.janicke.de

Janicke, U., and L. Janicke (2001): A three-dimensional plume rise model for dry and wet plumes. *Atmos. Environ.*, **35**:877-890.

Kaimal, J.C., Wyngaard, J.C., Haugen, D.A., Cote', O.R., Izumi, Y., Caughey, S.J. and Readings, C.J. (1976). Turbulence structure in the convective boundary layer. *J. Atmos. Sci.*, 33, 2152-2169.

Leahey, D.M., and M.J.E. Davies (1984): Observations of plume rise from sour gas flares. *Atmos. Environ.*, **18**:917-922.

Loh-Nien Fan (1967): Turbulent buoyant jets into stratified or flowing ambient fluids. Technical Report No. KH-R-15, California Institute of Technology, Pasadena, CA.

Luhar, A.K., and R.E. Britter (1992): Random walk modelling of buoyant-plume dispersion in the convective boundary layer. *Atmos. Environ.*, **26A**:1283-1298.

Manins, P.C. (1979): Partial penetration of an elevated inversion layer by chimney plumes. *Atmos. Environ*., **13**:733-741.

Manins, P.C. (1985): Cloud heights and stratospheric injections resulting from a thermonuclear war. *Atmos. Environ.*, **19**, 1245–1255

Manins, P.C., Carras J.N. and Williams D.L. (1992): Plume rise from multiple stacks. Clean Air, **26**, 65-68.

McGrattan K.B., Baum H.R. and Rehm R.G. (1996) Numerical simulation of smoke plumes from large oil fire. *Atmos. Environ.*, **30**:4125-4136

Moore, D.J. (1974): A comparison of the trajectories of rising buoyant plumes with theoretical/empirical models. *Atmos. Environ*., **8**:441-457.

Morton, B.R., G.I. Taylor, and J.S. Turner (1956): Turbulent gravitational convection from maintained and instantaneous sources. *Proc. Roy. Soc. London*, **A234**:1-23.

Netterville, D.D.J. (1990): Plume rise, entrainment and dispersion in turbulent winds. *Atmos. Environ*., **24**:1061-1081.

Nguyen K.C., Noonan J.A., Galbally I.E. and W.L. Physick (1997) Predictions of plume dispersion in complex terrain: Eulerian versus Lagrangian Models. *Atmos. Environ*., **31**:947-958.

Nieuwstadt, F.T., and J.P. de Valk (1987): A large-eddy simulation of buoyant and non-buoyant plume dispersion in the atmospheric boundary layer. *Atmos. Environ*., **21**:2573-2587.

Nieuwstadt, F.T.M. (1992a): A Large-Eddy Simulation of a Line Source in a Convective Atmospheric Boundary Layer - I. Dispersion Characteristics. *Atmos. Environ*., **26A**:485-495.

Nieuwstadt, F.T.M. (1992b): A Large-Eddy Simulation of a Line Source in a Convective Atmospheric Boundary Layer - II. Dynamics of a Buoyant Line Source. *Atmos. Environ*., **26A**:497-503.

Ooms, G. (1972): A new method for the calculation of the plume path of gases emitted by a stack. *Atmos. Environ.*, **6**: 899–909.

Ooms, G., A.P. Mahieu, and F. Zelis (1974): The plume path of vent gases heavier than air. *First International Symposium on Loss Prevention and Safety Promotion in the Process Industries*, The Hague, The Netherlands.

Ooms, G., and A.P. Mahieu (1981): A comparison between a plume path model and a virtual point source model for a stack plume. *Applied Scientific Research*, **36**: 339–356.

Overcamp T.J and Ku T. (1988): Plume rise from two or more adjacent stacks. *Atmos. Environ.*, **22**: 625–637.

Overcamp T.J (2001): A review of the conditions leading to downwash in physical modeling experiments. *Atmos. Environ.*, **35**: 3503–3508.

Physick, W.L. (1996) Photochemical smog studies in Australian cities. In: *Urban air pollution, volume 2*. H. Power, and N. Moussiopoulos (editors). Southhampton: Computational Mechanics Publications. p. 141–184.

Pierce, T.E., D.B. Turner, J.A. Catalano, and F.V. Hale (1982): PTPLU – A single source gaussian dispersion algorithm. User's Guide. Technical Report PB83-211235, U.S. Environmental Protection Agency, Environmental Sciences Research Laboratory, Research Triangle Park, NC.

Pope, S.B. (1994): On the Relationship between Stochastic Lagrangian Models of Turbulence and Second-Moment Closures. *Phys. Fluids*, **6**:973-985.

Priestley, C.H.B. (1956): A working theory of the bent-over plume of hot gas. *Quart. J. Roy. Met. Soc*., **82**, 165–176

Richards J.M. (1963): The penetration of interfaces by cylindrical thermals. *Quart. J. Roy. Met. Soc.,* **89,** 254-264

Risken, H. (1984): *The Fokker-Planck Equation.* Springer Verlag, Berlin, Heidelberg, New York.

Sandroni, S., P. Bacci, and D. Anfossi (1981): Aircraft observations of plume emitted from elevated sources. *Atmos. Environ*., **15**:95-100

Sawford, B.L. (1985): Lagrangian statistical simulation of concentration mean and fluctuating fields. *J. Climate Appl. Met*., 24, 1152-1166

Sawford, B.L. (1986): Generalized Random Forcing in Random-Walk Turbulent Dispersion Models. *Phys. Fluids*, **29**:3582-3585.

Schatzmann, M. (1979): An integral model of plume rise. *Atmos. Environ*., **13**:721-731.

Schatzmann, M., and A.J. Policastro (1984): An advanced integral model for cooling tower plume dispersion. *Atmos. Environ*., **18**:663-674.

Schulman, L.L., and J.S. Scire (1980): Buoyant line point source (BLP) dispersion model user's guide. Document P-7304-B, Environmental Research & Technology, Inc., Concord, MA.

Schulman, L.L., and S.R. Hanna (1986): Evaluation of downwash modifications to the Industrial Source Complex Model. *J. Air Pollut. Control Assoc.,* **36**:258-264.

Schulman, L.L., D.G. Strimaitis, and J.S. Scire (1997): Addendum to ISC3 user's guide. The PRIME plume rise and building downwash model. Electric Power Research Institute. http://www.epa.gov/scram001/

Schulman, L.L., D.G. Strimaitis, and J.S. Scire (2000): Development and evaluation of the PRIME plume rise and building downwash model. *J. Air Waste Manag. Assoc*., **50**:378-390.

Scire, J.S., and L.L. Schulmann (1980): Modeling plume rise from low-level buoyant line and point sources. Proceedings Second Point Conference on Applications of Air Pollution Meteorology, 24-28 March 1980, New Orleans, LA, 133-139.

Scire J.S., D.G. Strimaitis, and R.J. Yamartino (1999): A User's Guide for the CALPUFF Dispersion Model (Version 5.0). Technical Report. Earth Tech. Inc., 196 Baker Avenue, 01742 Concord, MA.

Shimanuki, A., and Y. Nomura (1991): Numerical simulation on instantaneous images of the smoke released from a chimney. *J. Met. Soc. Japan*, **69**:187-196.

Singer I.A. and Smith M.E. (1966): Atmospheric dispersion at Brookhaven National Laboratory. Int. J. Air Water Poll., **10**, 125

Slawson, P.R., and G.T. Csanady (1967): On the mean path of buoyant, bent-over chimney plumes. *J. Fluid Mech*., **28**:311-322.

Slawson, P.R., and G.T. Csanady (1971): The effect of atmospheric conditions on plume rise. *J. Fluid Mech.,* **47**:33-49.

Snyder, W.H., and R.E. Lawson Jr. (1991): Fluid modeling simulation of stack-tip downwash for neutrally buoyant plumes. *Atmos. Environ*., **12**:2837-2850.

Souto M.J., J.A. Souto, V. Perez-Munuzuri, J.J. Casares, and J.L. Bermudez (2001): A comparison of operational Lagrangian particle and adaptive puff models for plume dispersion forecasting. *Atmos. Environ.,* **35**:2349-2360.

Strom, G.H. (1976): *Transport and diffusion of stack effluents*. In: Stern, A.C. (editor) Air pollution, Vol.I. Academic Press, New York, USA.

Stuhmiller, J. (1974): Development and validation of a two-variable turbulence model. Science Applications, Inc., Report SAI-74-509-LJ, La Jolla, California.

Sutherland, V.C., and T.C. Spangler (1980): Comparison of calculated and observed plume rise heights for scrubbed and nonscrubbed buoyant plumes. Preprints, Second Joint Conference on Applications of Air Pollution Meteorology, New Orleans, American Meteorological Society, pp. 129-132.

Thomson, D.J. (1987): Criteria for the Selection of Stochastic Models of Particle Trajectories in Turbulent Flows. *J. Fluid Mech*., **180**:529-556.

Thompson, R.S., Snyder W.H. and Weil J.C. (2000): Laboratort simulation of the rise of buoyant thermals created by open detonation. *J. Fluid. Mech*., **417**: 127-156

Tinarelli, G., D. Anfossi, M. Bider, E. Ferrero, S. Trini Castelli (2000): A new high performance version of the Lagrangian particle dispersion model SPRAY, some case studies. Air Pollution Modelling and its Applications XIII, S.E. Gryning and E. Batchvarova eds., Kluwer Academic / Plenum Press, New York, 499-507. http://www.aria-net.it/PDF/e_spray3.pdf

Trelles J., K.B. McGrattan, H.R. Baum (1999a): Smoke transport by sheared winds. *Combust. Theory Modelling*, **3**:323-341.

Trelles J., K.B., McGrattan, H.R. Baum (1999b): Smoke dispersion from multiple fire plumes. *AIAA Journal*, **37**:1588-1601.

Turner, J.S. (1973): *Buoyancy effects in fluid.* Cambridge University Press, London.

Turner, D.B. (1985): Proposed pragmatic methods for estimating plume rise and plume penetration through atmospheric layers. *Atmos. Environ*., **7**:1215-1218.

Turner D.B., T. Chico and J.A. Catalano (1986) TUPOS - A multiple source gaussian dispersion algorithm using on site turbulence data. EPA Publication No. EPA - 600/8 - 86/010 U.S. Environmental Protection Agency, Research Triangle Park, North Carolina

U.S. Environmental Protection Agency (1995a): *SCREEN3 Model User's Guide.* Technical Report EPA-454/B-95-004. Research Triangle Park, NC.
http://www.epa.gov/scram001/

U.S. Environmental Protection Agency (1995b): *User's Guide for the Industrial Source Complex (ISC3) dispersion models. Volume II – description of model algorithms.* Technical Report A-454/B-95-003b. Research Triangle Park, NC. http://www.epa.gov/scram001/

U.S. Environmental Protection Agency (1998): *Revised draft user's guide for the AMS/EPA regulatory model – AERMOD.* Draft 11/10/98. http://www.epa.gov/scram001/

Vadot L. (1965): Study of diffusion of smoke plumes into the atmosphere (in French): Centre Interprofessionel Technique d'Etudes de la Pollution Atmospheric, Paris

van Dop, H., F.T.M. Nieuwstadt, and J.C.R. Hunt (1985): Random Walk Models for Particle Displacements in Inhomogeneous Unsteady Turbulent Flows. *Phys. Fluids*, **28**:1639-1653.

van Dop, H. (1992): Buoyant plume rise in a Lagrangian Framework. *Atmos. Environ*., **26A**:1335-1346.

van Haren, L., and F.T. Nieuwstadt (1989): The behaviour of passive and buoyant plumes in a convective boundary layer, as simulated with a large-eddy model. *J. Appl. Meteor*., **28**:818-832.

Yamada (2000) Numerical simulations of airflows and tracer transport in the southwestern United States. *J. Appl. Meteor*., **39**: 399-411.

Weil, J.C. (1974): The rise of moist, buoyant plumes. *J. Appl. Meteor*., **13**:435-443.

Weil, J.C. (1982): Source buoyancy effects in boundary layer diffusion. *Workshop on the parameterization of mixed layer diffusion*. R. Cionco (Ed.), Physical Science Laboratory, New Mexico State University, Las Cruces NM.

Weil, J.C. (1988): Plume Rise. In: *Lectures on Air Pollution Modeling*. A. Venkatram and J.C. Wyngaard, eds. American Meteorological Society, Boston, 119-166.

Weil J.C. (1994) A hybrid Lagrangian dispersion model for elevated sources in the convective boundary layer. *Atmos. Environ.*, **28**:3433-3448.

Weil J.C., L.A. Corio, and R.P. Brower (1997). APDF dispersion model for buoyant plumes in the convective boundary layer. J. Appl. Meteoror., **36**, 982-1003.

Wigley, T.M., and P.R. Slawson (1975): The effect of atmospheric conditions on the length of visible cooling tower plumes. *Atmos. Environ*., **9**:437-445.

Willis G. and J. Deardorff (1983): On plume rise within a convective boundary layer. *Atmos. Environ.*, **17**:2435-2447.

Willis G. and J. Deardorff (1987). Buoyant plume dispersion and entrapment in and above a laboratory mixed layer, *Atmos. Environ.*, **21**:1725-1735.

Zannetti, P., and N. Al-Madani (1983): Numerical simulations of Lagrangian particle diffusion by Monte-Carlo techniques. VIth World Congress on Air Quality (IUAPPA), Paris, France, May 1983.

Zannetti, P., and N. Al-Madani (1984): Simulation of transformation, buoyancy and removal processes by Lagrangian particle methods. Proceedings of the 14th International Technical Meeting on Air Pollution Modelling and its Application (ed. Ch. de Wispelaere) Plenum Press, New York, 733-744.

Zannetti, P. (1990): *Air pollution modeling: theories, computational methods and available software.* Computational Mechanics Publications. Van Nostrand Reinhold, New York.

Zhang, X., and A.F.A. Ghoniem (1993): Computational Model for the Rise and Dispersion of Wind-Blown, Buoyancy Driven Plumes - I. Neutrally Stratified Atmosphere. *Atmos. Environ*., **27A**:2295-2311.

Zhang, X., and A.F.A. Ghoniem (1994a): Computational Model for the Rise and Dispersion of Wind-Blown, Buoyancy Driven Plumes - II. Linearly Stratified Atmosphere. *Atmos. Environ*., **28**:3005-3018.

Zhang, X., and A.F.A. Ghoniem (1994b): Computational Model for the Rise and Dispersion of Wind-Blown, Buoyancy Driven Plumes - III. Penetration of Atmospheric Inversion. *Atmos. Environ*., **28**:3019-3032.